

**NUCLEAR MODEL CALCULATION OF EXCITATION FUNCTIONS OF  
NEUTRON INDUCED REACTIONS ON THE STRUCTURAL MATERIALS  
OF THE MINIATURE NEUTRON SOURCE REACTOR.**

**BY**

**DAUDA ALIYU**

**Msc/Scie/51710/05-06**

**A THESIS SUBMITTED TO THE POST GRADUATE SCHOOL  
AHMADU BELLO UNIVERSITY, ZARIA, NIGERIA**

**IN PARTIAL FULFILMENT OF THE REQUIREMENTS FOR THE AWARD OF  
THE DEGREE OF MASTER OF SCIENCE IN PHYSICS (NUCLEAR OPTION)  
DEPAERTMENT OF PHYSICS AHMADU BELLO UNIVERSITY ZARIA.**

**MARCH 2011**

## **DECLARATION**

I hereby declare that the report in this thesis is the result of my original research. This thesis has not been submitted to any other institute, organizations, or body for any award other than Ahmadu Bello University, Zaria, Nigeria.

All inclusion from works other than this have been referenced and acknowledged.

-----  
**Aliyu Dauda**

-----  
**Date**

## CERTIFICATION

This thesis titled **NUCLEAR MODEL CALCULATION OF THE EXCITATION FUNCTIONS OF NEUTRON INDUCED REACTIONS ON THE STRUCTURAL MATERIALS OF THE MINIATURE NEUTRON SOURCE REACTOR** by Aliyu Dauda meets the regulation governing the awards of the Degree of Master of Science (Physics) of Ahmadu Bello University, Zaria, Nigeria and is approved for its contribution to knowledge and literary presentation.

-----  
Prof. S.A. Jonah  
(Chairman Supervisory Committee)

-----  
Date

-----  
Dr. G.I. Balogun  
(Member Supervisory Committee)

-----  
Date

-----  
Dr. N. Rabi  
Head Department of Physics

-----  
Date

-----  
Prof Joshua Adebayo Abiodun  
Dean Postgraduate School

-----  
Date

## **DEDICATION**

This work is dedicated to my late mother Hajiya Aishatu Dauda Aliyu (May Almighty Allah Grant her Aljanatu Firdaus Ameen).

## **ACKNOWLEDGMENTS**

I wish to express my sincere gratitude to my parents, Alhaji Dauda Aliyu and late Hajiya Aishatu Dauda Aliyu, my sisters and my brothers. I'll long appreciate your many kind and thoughtful deeds. I thank you from the bottom of my heart for all your treasured wisdom and the warmth that you care. My future's bright through the fine example of your love.

My unfeigned appreciation to my friends who stood by me, guided me, and gave me affectionate companionship.

A special commendation goes to my supervisors Prof. S.A. Jonah and Dr G.I Balogun, for their guidance. Their efforts in making sure I do the right things are worth mentioning. I will also thank all my lecturers and colleagues from whom I learned a lot.

Only God can reimburse them for what they've thought me. Once again, I thank you.

May God bless us all, bountifully

## ABSTRACT

Nuclear models calculation of excitation functions was performed using the nuclear theoretical model code EXIFON on the impurity nuclides of the Be-reflector of the MNSR (NIRR-1) elements with concentration greater than 100ppm were considered in the energy range of 0-20MeV. Result of the calculated excitation functions obtained with the code EXIFON were compared with the experimental data retrieved from IAEA-Nuclear Data section EXFOR data library. Some of the results of the calculated excitation functions agree well with the experimental data, while some disagree. The good agreement was obtained for nuclides with magic number of neutrons and protons. Shell structure effects were not taken into consideration during calculation with theoretical model code. This might be the reason for disagreement. It is also noted that most of the data retrieved from EXFOR data library were incomplete, scanty, and are measured around 14MeV. This exposed the short coming of using measured data for calculation of excitation functions. On the other hand the result of calculated excitation function with the Code EXIFON seems to give good result.

## TABLE OF CONTENT

Title page:	-	-	-	-	-	-	-	-	-	-	i
Declaration:-	-	-	-	-	-	-	-	-	-	-	ii
Certification:	-	-	-	-	-	-	-	-	-	-	iii
Dedication: -	-	-	-	-	-	-	-	-	-	-	iv
Acknowledgement:	-	-	-	-	-	-	-	-	-	-	v
Abstract: -	-	-	-	-	-	-	-	-	-	-	vi
Table of content:	-	-	-	-	-	-	-	-	-	-	vii

### CHAPTER ONE: INTRODUCTION AND BACKGROUND OF THE STUDY

1.1	Statement of the Problem:	-	-	-	-	-	-	-	-	-	2
1.2	Justification of the Research Work	-	-	-	-	-	-	-	-	-	2
1.3	Purposes of the Research	-	-	-	-	-	-	-	-	-	3
1.4	Previous Work	-	-	-	-	-	-	-	-	-	4
1.5	Present Work-	-	-	-	-	-	-	-	-	-	5
1.6	Theoretical Consideration	-	-	-	-	-	-	-	-	-	6

### CHAPTER TWO: LITERATURE REVIEW

2.0	NIGERIA RESEARCH REACTOR-1 (NIRR-1)	-	-	-	-	-	-	-	-	-	9
2.1:	MODELS OF NUCLEON INDUCED REACTION	-	-	-	-	-	-	-	-	-	11
2.1.1:	Cross Sections.	-	-	-	-	-	-	-	-	-	12
2.1.2:	Direct Process	-	-	-	-	-	-	-	-	-	12
2.1.3:	Compound Nuclear Reaction	-	-	-	-	-	-	-	-	-	12
2.1.4:	Optical model	-	-	-	-	-	-	-	-	-	18
2.1.5:	Derivation	-	-	-	-	-	-	-	-	-	18
2.2:	Types of Nuclear Model Codes	-	-	-	-	-	-	-	-	-	19
2.2.1:	Empire	-	-	-	-	-	-	-	-	-	19

2.2.2	Statistical Multi Step Code EXIFON	-	-	-	-	-	-	-	21
2.2.3:	Activation Cross Section	-	-	-	-	-	-	-	21
2.2.4:	Angular Distributions	-	-	-	-	-	-	-	22
2.2.5:	The SMD Cross Section	-	-	-	-	-	-	-	23
2.2.6:	SMC Cross Section (Basic Formula)	-	-	-	-	-	-	-	23
2.2.7:	SMC Formation Cross – Section	-	-	-	-	-	-	-	23
2.2.8:	Multiple Particles Emission (MPE)	-	-	-	-	-	-	-	23
2.3	NUCLEAR DATA TYPES AND DATA CENTERS	-	-	-	-	-	-	-	24
2.3.1:	The role of the IAEA nuclear data section	-	-	-	-	-	-	-	24
2.3.2:	Nuclear data types	-	-	-	-	-	-	-	24
2.3.4:	Bibliographic data	-	-	-	-	-	-	-	25
2.3.5	Experimental data	-	-	-	-	-	-	-	25
2.3.6	Evaluated data	-	-	-	-	-	-	-	25
2.3.7	Data access and service	-	-	-	-	-	-	-	26
CHAPTER THREE: MATERIALS AND METHOD									
3.0:	Material and Method	-	-	-	-	-	-	-	27
3.1:	(n.p) Reaction	-	-	-	-	-	-	-	27
3.2:	(n. $\alpha$ ) Reaction	-	-	-	-	-	-	-	29
3.3:	INSTALLATION AND RUNNING OF EXIFON CODE	-	-	-	-	-	-	-	30
3.3.1:	Standard Parameter Set	-	-	-	-	-	-	-	31
3.3.2:	Modifications	-	-	-	-	-	-	-	31
3.3.3:	Input Data File	-	-	-	-	-	-	-	32
3.3.4:	OUTPUT DATA FILE	-	-	-	-	-	-	-	34
3.4:	EXFOR DATA LIBRARY RETRIEVAL	-	-	-	-	-	-	-	35
3.4.1:	Access to EXFOR Library	-	-	-	-	-	-	-	36

## CHAPTER FOUR: RESULT AND DISCUSSION

4.0	RESULTS AND DISCUSSION	-	-	-	-	-	-	-	37
4.1.	Fe Nuclides.	-	-	-	-	-	-	-	37
4.2.	Al Nuclides	-	-	-	-	-	-	-	40
4.3.	Si Nuclides	-	-	-	-	-	-	-	41
4.4.	Cu Nuclides	-	-	-	-	-	-	-	43
4.5	N Nuclides	-	-	-	-	-	-	-	45
4.6	Cr Nuclides	-	-	-	-	-	-	-	46
4.7	Zn Nuclides	-	-	-	-	-	-	-	48
4.8	Ni Nuclides.	-	-	-	-	-	-	-	50
4.9	Pb Nuclides	-	-	-	-	-	-	-	53
4.10	Mg Nuclides	-	-	-	-	-	-	-	54
4.11	Co Nuclide	-	-	-	-	-	-	-	57
4.12	Mn Nuclide	-	-	-	-	-	-	-	58
4.13	O Nuclides	-	-	-	-	-	-	-	59

## CHAPTER FIVE: CONCLUSIONS AND RECOMMENDATIONS

5.0:	CONCLUSION:	-	-	-	-	-	-	-	63
5.1:	RECOMMENDATIONS:	-	-	-	-	-	-	-	64
	References	-	-	-	-	-	-	-	65

## LIST OF TABLES

Table 1: Summary of the status of calculated excitation

functions using EXIFOR and EXIFON - - - - - 61

## LIST OF FIGURES

Figure 1: Vertical cross section of NIRR-1	-	-	-	-	-	-	10
Figure 2: Floor process within the reactor core	-	-	-	-	-	-	11
Figure 4.1a FE54(n,p) reaction	-	-	-	-	-	-	38
Figure 4.1b FE56(n,p) reaction	-	-	-	-	-	-	38
Figure 4.1c FE57(n,p) reaction	-	-	-	-	-	-	39
Figure 4.1d FE54(n, $\alpha$ ) reaction	-	-	-	-	-	-	39
Figure 4.1e FE56(n, $\alpha$ ) reaction	-	-	-	-	-	-	40
Figure 4.2a Al27(n, $\alpha$ ) reaction	-	-	-	-	-	-	41
Figure 4.2b Al27(n,p) reaction	-	-	-	-	-	-	41
Figure 4.3 Si28(n,p) reaction	-	-	-	-	-	-	42
Figure 4.3b Si30(n, $\alpha$ ) reaction	-	-	-	-	-	-	42
Figure 4.3c Si30(n,p) reaction	-	-	-	-	-	-	43
Figure 4.4a Cu63(n, $\alpha$ ) reaction	-	-	-	-	-	-	44
Figure 4.4b Cu65(n, $\alpha$ ) reaction	-	-	-	-	-	-	44
Figure 4.4c Cu65(n,p) reaction	-	-	-	-	-	-	45
Figure 4.4d Cu63(n, $\alpha$ ) reaction	-	-	-	-	-	-	44
Figure 4.5a N4(n,p) reaction	-	-	-	-	-	-	45
Figure 4.6a Cr50(n,p) reaction	-	-	-	-	-	-	46
Figure 4.6b Cr52(n,p) reaction	-	-	-	-	-	-	47
Figure 4.6c Cr53(n,p) reaction	-	-	-	-	-	-	47
Figure 4.6d Cr54(n,p) reaction	-	-	-	-	-	-	47
Figure 4.6e Cr54(n, $\alpha$ ) reaction	-	-	-	-	-	-	48
Figure 4.7a Zn64(n,p) reaction	-	-	-	-	-	-	48
Figure 4.7b Zn68(n,p) reaction	-	-	-	-	-	-	49
Figure 4.7c Zn66(n,p) reaction	-	-	-	-	-	-	49
Figure 4.7d Zn64(n, $\alpha$ ) reaction	-	-	-	-	-	-	50
Figure 4.7e Zn68(n, $\alpha$ ) reaction	-	-	-	-	-	-	50
Figure 4.8a Ni58(n,p) reaction	-	-	-	-	-	-	51

Figure 4.8b Ni58(n, $\alpha$ ) reaction	-	-	-	-	-	-	51
Figure 4.8c Ni60(n,p) reaction	-	-	-	-	-	-	52
Figure 4.8d Ni62(n, $\alpha$ ) reaction	-	-	-	-	-	-	52
Figure 4.8e Ni61(n,p) reaction	-	-	-	-	-	-	53
Figure 4.9a Pb206(n, $\alpha$ ) reaction	-	-	-	-	-	-	54
Figure 4.9b Pb208(n,p) reaction	-	-	-	-	-	-	54
Figure 4.10a Mg24(n,p) reaction	-	-	-	-	-	-	55
Figure 4.10b Mg25(n,p) reaction	-	-	-	-	-	-	55
Figure 4.10c Mg24(n, $\alpha$ ) reaction	-	-	-	-	-	-	55
Figure 4.10d Mg26(n, $\alpha$ ) reaction	-	-	-	-	-	-	56
Figure 4.10e Mg25(n, $\alpha$ ) reaction	-	-	-	-	-	-	56
Figure 4.11a Co59(n,p) reaction	-	-	-	-	-	-	57
Figure 4.11b Co59(n, $\alpha$ ) reaction	-	-	-	-	-	-	57
Figure 4.12a Mn55(n,p) reaction	-	-	-	-	-	-	58
Figure 4.12b Mn55(n, $\alpha$ ) reaction	-	-	-	-	-	-	59
Figure 4.13a O16 (n, $\alpha$ ) reaction	-	-	-	-	-	-	59
Figure 4.13b O17 (n, $\alpha$ ) reaction	-	-	-	-	-	-	60

## List of graphs

## CHAPTER ONE

### 1.0 INTRODUCTION AND BACKGROUND OF THE STUDY

Research reactors have played a significant role in the development of scientific and technical infrastructure in many countries. In developing countries, low power research reactors are acquired for training and research aimed at the introduction of Nuclear Power technology. (Jonah *et al*, 2005). In Nigeria, the first nuclear research reactor, a Miniature Neutron Source Reactor (MNSR) code named Nigeria Research Reactor -1 (NIRR-1) is sited at CERT, ABU. Presently, there are eight commercial Miniature Neutron Source Reactors (MNSR) in the world and Nigeria Research Reactor – 1 (NIRR-1) which went critical for the first time on February 03, 2004 is the eighth. The core of NIRR-1 with a fuel enrichment of over 90% was designed to last for approximately 10 years (Balogun *et al* 1999). Frequent refueling is avoided by the addition of Beryllium shims (Be) to compensate for the fuel burn up and long time poisoning effect. To achieve efficient shimming, the commercial (MNSR) has been designed with an atomic H/U<sup>235</sup> ratio of 197 in the fuel lattice leading to further core under moderation (Jonah *et al* 2005). As expected, there is enhanced contribution from fission neutron at the irradiation channel, via threshold reaction on the Be shim serving as a reflector. Fe, Al, N, Mg, Si, Ni, Zn, Cu, Cr, with concentration greater than 100 ppm (part per million), impurities are known to be present in the Be – reflector of the MNSR(SAR,2005). The life time of the structural materials of the MNSR is put at 20 years by the manufacturer, during which this impurity elements are exposed to neutrons of energy between 0 to 20 MeV. Nuclear transmutation induced by these energetic neutrons causes damage in the material. The knowledge of cross section data due to ( $n$ ,

$p$ ) and  $(n, \alpha)$  reaction on these elements could give information on the helium and hydrogen gas formation in the reflector. Finally, presence of these significant amount of impurities in the Be – reflectors can cause possible long – lived induced radioactivity of the structural material irradiated for 20 years or more (use time of the radiation) from radio nuclides of Ca , Fe , Co , Cs and Eu which are responsible for long-lived activity.

### **1.1 Statement of the problem**

The research intends to address the following problems:

- Impurities (Fe, Al, Mg, Si, Ni, Zn, Cu, Cr, O, N, Mn, Pb, Co with concentration > 100ppm) are found to be present in the Be – reflector of the MNSR (Jonah *et al.*, 2005).
- Impurity elements exposed to neutrons of energy between 0 to 20MeV could cause damage to the structural material of the MNSR, via nuclear transformation.
- Information on the helium and hydrogen gas formation on the Be –reflector as a result of nuclear transmutations, that could cause possible damage to the structure of the Beryllium shim and the Reactor in general.
- Experimental cross section data of some of these elements in the energy range of 0 – 20Mev are incomplete and discrepant, so also are recommended data.

### **1.2 Justification of the Research Work**

The NIRR-1 is a low power nuclear research reactor which has highly enriched uranium as a fuel, light water as moderator, and Be-shims as reflector. The following

element are the major impurities-in the Be reflector of the MNSR with concentration greater than 10ppm which include Fe 4000ppm, Mg 1000ppm, Al 3000ppm, Si 800ppm, Cu 200ppm, N 200ppm, Cr 200ppm, Zn 150ppm, Ni 100ppm, Pb 30ppm, Co 100ppm, Mn 200ppm and Oxygen in (BeO) 2500ppm (Jonah *et al*, 2005).

1. Hence, it is interesting to investigate the formation of various nuclides of the impurities via  $(n,\alpha)$  and  $(n, p)$  reaction and result of their exposure to neutrons of energy between 0 – 20MeV, which could give account of the integrity of the structural material of the MNSR, *i.e.* Be-reflector.
2. Nuclear transmutation induced by these energetic neutrons cause damage in the materials, most especially, the knowledge of the reaction cross section data due to  $(n,\alpha)$  and  $(n,p)$  reaction on these element could give information on Helium and Hydrogen gas formation respectively on the Be-reflector.
3. Long-lived induced radioactivity of the structural materials irradiated for 20years or more (*i.e.* life time of the reactor) and cooled for more than one year. Such radio Nuclides as Ca, Fe, Cu, Cs, and Eu are responsible for the long-lived activity in the Be-reflector. The concentration of the above element and activation cross section data should be taken into consideration, even at the stage of reactor design and during de-commissioning of the reactor.

### **1.3 Purposes of the Research**

The purpose of this research work is to achieve the following;

1. To use Nuclear model of statistical multi-step direct and multistep compound (SMD and SMC) for calculation of excitation function  $(n, \alpha)$  and  $(n, p)$  reaction for impurities in the Be-reflector.
2. To compare the calculated results of the excitation functions  $(n, p)$  and  $(n, \alpha)$  reactions induced on the impurities of Be-reflector with the experimental value in the EXFOR DATA library, in order to test the suitability of the model used.
3. To use the experimental data to investigate the suitability of the theoretical models upon which the EXIFON is based for elements of interest.
4. Experimental cross section data of some of these elements in the energy range of 0 – 20MeV are incomplete and discrepant, so theoretical calculation of excitation function can assist in the provision of cross section data.

#### 1.4. Previous Work

The energy and angular distribution of pre-equilibrium nucleon from 14MeV neutron energy with target Nuclei  $^{51}\text{V}_i$  to  $^{58}\text{N}_i$  are analyzed by multi-step compound (MSC) theory formalism of Feshback, Kerman and Koonin (FKK) and Geometry Dependent Hybrid (GDH) model by M. Avrigeanu and P.E. Hudgson in 1992. The same parameter set were used for both of these calculation with no free parameter, the calculations are compared with experimental data and the applicability of theory assessed.

Similar work was carried out by Jonah 2004, for the use of shell structure effect in neutron cross section calculations by theoretical model code. Others are inelastic scattering of neutron using statistical model by Walter Hauser and Herman Feshback (1952) and statistical multi-step reaction model for nuclear data by H. Kalka in (1991).

### 1.5. Present Work

In this work, the nuclear model calculation of excitation function will be based on the 'EXIFON' code and will be performed to determine the activation cross section data for  $(n, p)$  and  $(n, \alpha)$  reaction, with neutron incident energy from  $(0 - 20\text{MeV})$ , in step of  $2\text{MeV}$  on the impurities in the Be reflector. This will be done for impurity elements  $^{54}\text{Fe}$ ,  $^{55}\text{Fe}$ ,  $^{56}\text{Fe}$ ,  $^{57}\text{Fe}$ ,  $^{24}\text{Mg}$ ,  $^{25}\text{Mg}$ ,  $^{26}\text{Mg}$ ,  $^{27}\text{Al}$ ,  $^{28}\text{Si}$ ,  $^{29}\text{Si}$ ,  $^{30}\text{Si}$ ,  $^{58}\text{Ni}$ ,  $^{60}\text{Ni}$ ,  $^{61}\text{Ni}$ ,  $^{62}\text{Ni}$ ,  $^{63}\text{Ni}$ ,  $^{14}\text{N}$ ,  $^{15}\text{N}$ ,  $^{63}\text{Cu}$ ,  $^{65}\text{Cu}$ ,  $^{55}\text{Mn}$ ,  $^{64}\text{Zn}$ ,  $^{66}\text{Zn}$ ,  $^{67}\text{Zn}$ ,  $^{68}\text{Zn}$ ,  $^{70}\text{Zn}$ ,  $^{50}\text{Cr}$ ,  $^{52}\text{Cr}$ ,  $^{53}\text{Cr}$ ,  $^{54}\text{Cr}$ ,  $^{59}\text{Co}$ ,  $^{16}\text{O}$ ,  $^{17}\text{O}$ ,  $^{18}\text{O}$ ,  $^{204}\text{Pb}$ ,  $^{206}\text{Pb}$ ,  $^{207}\text{Pb}$ ,  $^{208}\text{Pb}$ , base on the isotopic abundance.

The analytical model is statistical multi step code which is based on many body theory and the random matrix physics. It utilized the statistical multi step direct and multi step compound reaction for the prediction of emission spectra, angular distribution and activation cross section taking into account equilibrium, pre-equilibrium as well as direct processes. It is a fast code which predicts the cross section data from global parameter set, in order to access the excitation functions of the impurity element. Detailed description of the model used in the 'EXIFON' code has been given in a report by H. Kalka (1991) and Kalka *et al* (1990).

## 1.6. THEORETICAL CONSIDERATION

At low energies of incoming particles and for the majority of nuclear system, nuclear reaction occur on two distinct time scales, the one that occurs promptly in a time scale of approximately  $10^{-22}$  S, is called direct reaction, while the one involving quasi-bound intermediate complex system is called compound nuclear reaction takes place in a time scale approximately  $10^{-14}$  S. The compound nuclear model utilizing the Hauser-Feshbach statistical approach (Hauser-Feshbach 1952) is the basis of which majority of the codes for cross section calculation at projectile energies  $300\text{MeV}$  are written (Jonah *et al* 2005).

In this approach the interaction of the incident particle with a target nucleus proceeds by the formation of a system of compound nucleus, there after, the system breaks up into possible reaction channels consisting of one, two or more nuclei of nuclides having various internal and relative states as depicted in the figure below.

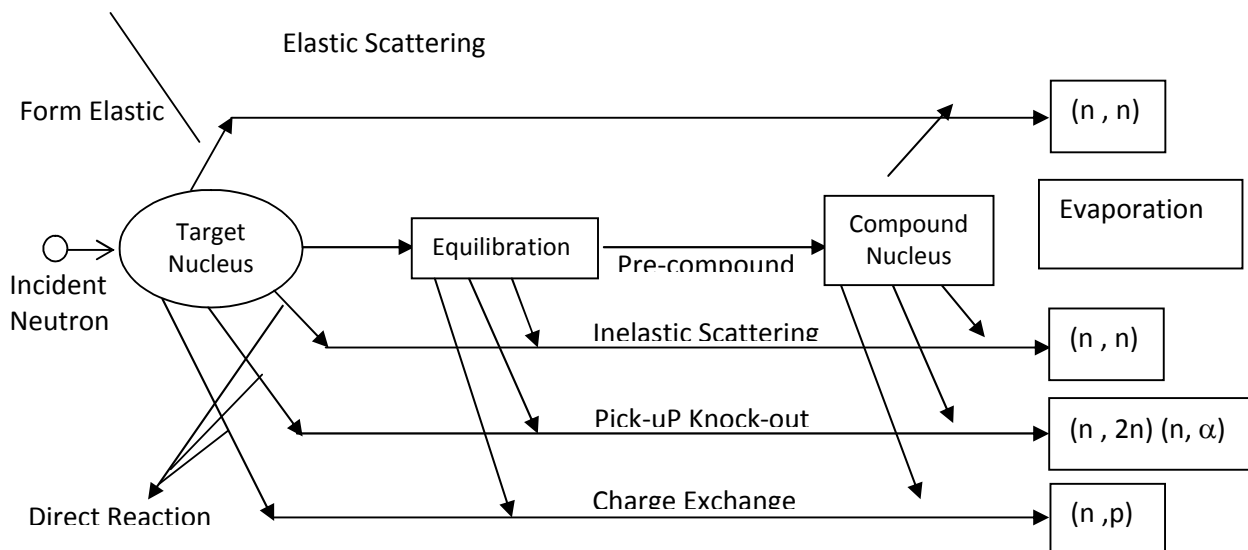


**Fig. Showing Schematic Diagram of Neutron Nucleus Interaction reaction**

In this work, the code 'EXIFON' which is based on the formalism of statistical multistep reaction model is used to performed the calculation of the excitation function of impurities in the Be-reflector; by considering threshold reaction *via* (n,p) and (n, $\alpha$ ) reactions in energy range of 0 – 20MeV. In step of 2MeV, at each projectile (neutron) energies.

In order to calculate the excitation function of impurities in the Be-reflector, a simple two body interaction is assumed and the single state particle density of particle (n,p, $\alpha$ ) with reduced mass U is given by

$$g = 4\rho(E_F)$$

Where the factor 4 takes into cognizance the spin and isospin degeneracy

$$\rho(E_F) = (4.8 \times 10^{-3} F_m^{-3} MeV^{-3/4}) r_0^3 A E^{1/2}$$

Other global parameters set for the excitation function are:

$$\text{Strength of delta-interaction } F_0 = 27.5 MeV$$

$$\text{Radius parameter } r_0 = 1.21 + 4.0A^{-2/3} \approx 15A^{-4/3} Fm$$

$$\text{Potential depth } V_0 = 52.03 MeV$$

$$\text{Fermi energy } E_F = 33 MeV$$

$$\text{Paring shift } A = 12.8A^{-1/2} MeV$$

$$\text{Phonon (Breit } \square \text{ Wigner) width } \Delta_w = 1.4 MeV$$

Optical model Wilmore □Hodgson for neutron

Huizenga – Igo for alphas ( $\alpha$ ), Perey *et al* for protons. Detail description of the model use in EXIFON code has been given in literature review. (H. Kalka 1990).

The measured data will be retrieved from the EXFOR data library issued in 2003 by nuclear data section (NDS) of the I.A.E.A. The EXFOR data library consists of experimental nuclear reaction data induced by Neutron, charged particles and photons as reported in the literature by different authors. It is compiled continuously by the Network of nuclear reaction data centre around the globe and coordinated by the NDS. The library contains Neutron, charged particles – induced and photo nuclear data including integral and all types of differential cross section; resonance parameters, polarization data, fission yields and many other related data. Both numerical data tables and a structured abstract with experimental and bibliographic information are equally provided.

## CHAPTER TWO:

### LITERATURE REVIEW

#### 2.0 NIGERIA RESEARCH REACTOR-1 (NIRR-1)

Nigeria Research Reactor-1 (NIRR-1) is a Miniature Neutron Source Reactor. (MNSR) designed by China Institute of Atomic Energy (CIAE) (Zhoy Yongmao, 1986). First criticality was achieved on 03 February 2004 and has been operated safely (Jonah et al 2006). It is specifically designed for use in Neutron Activation Analysis (NAA) and limited radio isotope production. NIRR-1 has a tank in pool structural configuration and a nominal thermal power rating of 31kw. The current core of the reactor is 230 x 230mm square cylinder and fueled by U – Al<sub>4</sub> enriched to (90% in Al-alloy cladding). It has a total number of 347 fuel pins and three A<sub>1</sub> dummies in the fuel lattice. The length being 230mm with 9mm A<sub>1</sub>-alloys plug at each end. The diameter of the fuel meat is 4.3mm and the <sup>235</sup>U loading in each fuel element is about 2.88g. The cladding is A<sub>L</sub>-alloy, whose thickness is 0.6mm. There is only one control rod (CR) in NIRR-1 serving as shim rod, regulation rod as well as safety rod. The functions of the reactor starts up, and shut down are accomplished by moving the control rod. The CR is made up a cadmium absorber 266mm long 3.9mm in diameter, with stainless steel of 0.5mm thickness as the cladding material. The overall length of CR, is 450mm in length. A detailed description of the highly enriched uranium (HEU) core can be found in the final safety analysis report (SAR) (SAR 2005).

With a built-in clean cold core excess reactivity of 3.77mk measured during the on-site zero power and criticality experiments, the reactor can operate for a maximum of

4.5hrs at full power, mainly due to the large negative temperature feedback effects. Under this conditions with the same fuel loading, the reactor can run for over 10years with a burn-up of >1% (SAR 2005).

Prior to its commissioning, some Neutronics parameters have been calculated using a combination of WIMS and CITATION Code (Balogun 2003).

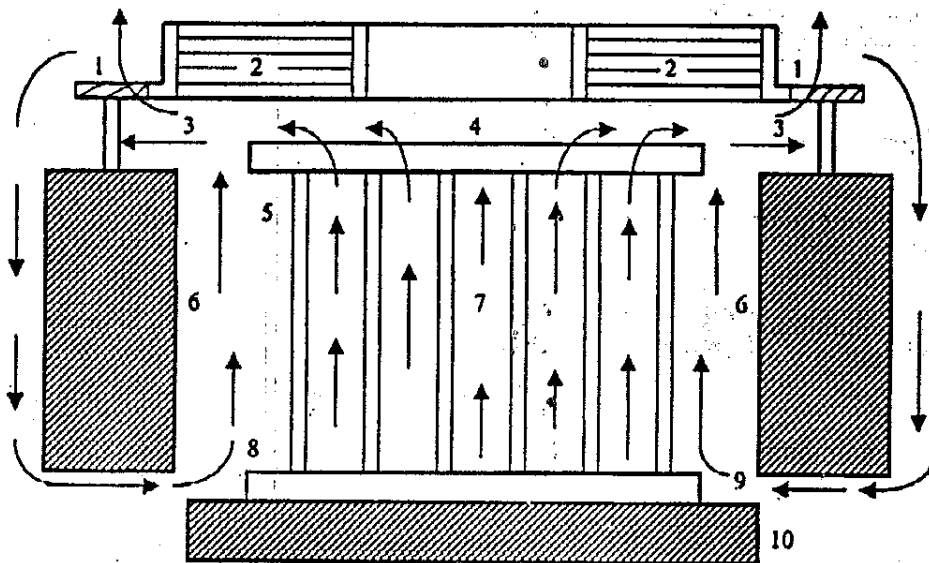


**Fig.1: Shows Vertical Cross Section of NIRR-1**

**Key:**



- |                          |                            |                            |
|--------------------------|----------------------------|----------------------------|
| 1 = 1 Top plate          | 2 = Top be reflector shims | 3 = Upper orifice          |
| 4 = Top fuel grid plate  | 5 = fuel element           | 6 = 6 Annular be reflector |
| 7 = Reactor core         | 8 = Bottom fuel grid plate | 9 = Lower orifice          |
| 10 = Bottom be reflector | Direction of coolant flow. |                            |

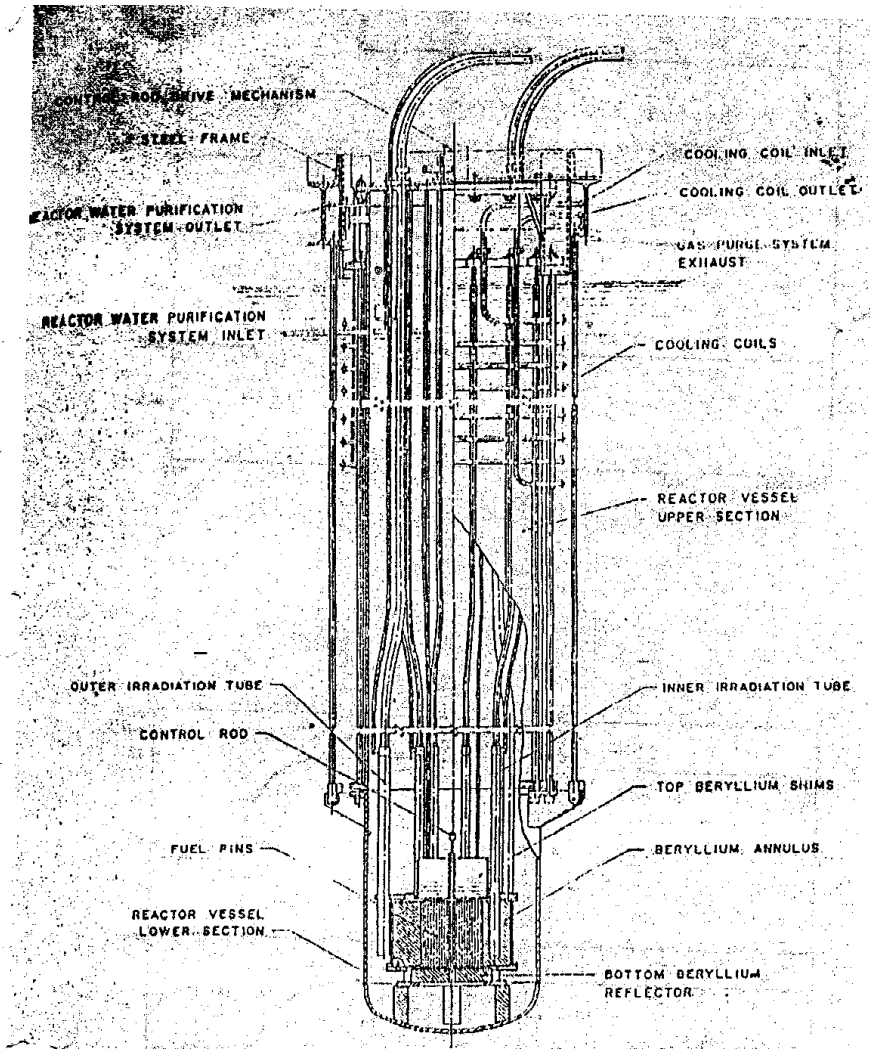


**Fig.2: Floor process within the reactor core**

**2.1: MODELS OF NEUTRON INDUCED REACTION**

A Nuclear reaction is initiated when a Nucleon or Nucleus collides with another nucleon of nucleus. Reactions are characterized in the first place by incoming nuclei and the outgoing reactions.

### **2.1.1: Cross Sections.**

The characteristic and the reaction induced by a given pair of incident Nucleon/nuclei can be summarized in distribution of the occurrence of the reaction product called cross sections denoted by  $\sigma_p$  for the production of a given product p is defined as:

$$\sigma_p = \frac{\text{No. of particles P produced per unit time}}{\text{No. of incident particle per unit time per unit area}} \quad - \quad (1)$$

### **2.1.2: Direct Process**

Direct reaction occurs promptly on a time scale of the same magnitude as time it takes the projectile nucleus to pass by the target nucleus. It occurs on a time scale approximately  $10^{-22}$  second.

### **2.1.3: Compound Nuclear Reaction**

Compound Nuclear Reaction which involved the formation of a quasi-bound intermediate, complex, occur on a time scale that is at least several order of magnitude larger i.e.  $10^{-14}$ S.

The contribution of direct reactions to the cross sections varies smoothly with energy. Compound Nuclear reaction makes contributions to the cross section that fluctuates rapidly with energy known as Resonances.

For example, a neutron incident on  $^{58}\text{Ni}$  nucleus to form  $^{58}\text{Ni}+n$  or  $^{59}\text{Ni}$ . One can observe direct reaction cross section – result of elastic scattering of the neutron. In this case and a compound nuclear state of  $^{59}\text{Ni}$  which is demonstrated by a faster variation of cross section with energy.

To separate direct and compound nucleus contribution to scattering one begins by partitioning of Hilbert space of state into components  $^1P$  is containing the prompt state and orthogonal component  $^1Q$  contains the closed channels of the intermediate compound complex.

Let  $^1P$  be subspace consisting a nucleon scattering of  $^{58}\text{Ni}$ , while  $^1Q$  consist of ground and excited state of nucleus  $^{59}\text{Ni}$ , (other process such as emission or heavier nuclear fission)

The projection of operators  $P$  and  $Q$  onto its Subspace  $^1P$  and  $^1Q$  respectively

$$P = P^\dagger \quad Q = Q^\dagger \quad - \quad (2)$$

$$P^2 = P \quad Q^2 = Q$$

$$P + Q = 1$$

They are then used to decompose the state vector of the system  $\psi$ . and its Schrödinger equation.

$$[E - H ]\psi = 0 \quad - \quad (3)$$

The prompt component of the state vector is  $P\psi$ , while the slower component is  $Q\psi$  With

$$\psi = P\psi + Q\psi \quad - \quad (4)$$

Multiplying equation (3) on the left by P or Q and use, the decomposition of the wave vector to write the equation as two coupled equations

$$[E - H_{pp}] P\psi = V_{pQ} Q\psi \quad - \quad (5)$$

$$\text{and } [E - H_{QQ}]Q\psi = V_{QP} P\psi \quad -(6)$$

Where  $H_{pp} \equiv H_0P + V_{pp} \equiv PH_0P + PVP$

$$V_{pQ} = PHQ \text{ etc}$$

With the assumption that the contributions to the Hamiltonian of internal degrees of freedom and kinetic energy both contain in  $H_0$  do not couple the 'P and 'Q subspace.

We may solve formally for these equation (5) as

$$P\psi_c = \Phi_c^{(+)} + \frac{1}{E(+)-H_{pp}} V_{pQ} Q\psi_c \text{-----}(7)$$

In which (+) denotes an incoming wave boundary condition the vector  $\Phi_c^{(+)}$  satisfies the Schrödinger equation in the 'P subspace.

$$[E - H_{pp}]\Phi_c^{(+)} = 0 \quad - \quad (8)$$

With an incoming wave channel c alone (and none in the Q subspace)and  $P\psi_c$  and  $Q\psi_c$  are the component of the full wave vector that evolve from this incoming wave. The solution  $P\psi_c$  when substituted into the second coupled equation (6) yields

$$[E - H_{QQ} - W_{QQ}]Q\psi_c = V_{QP} \Phi_c^{(+)} \text{-----} (9)$$

Where  $W_{QQ} \equiv V_{QP} \frac{1}{E^{(+)} - H_{PP}} V_{PQ}$  ----- (10)

To decompose the P' subspace Greens function into its real and imaginary part as:

$$\frac{1}{E^{(+)} - H_{PP}} = \frac{P.P}{E.H_{PP}} - i\pi\delta(E - H_{PP})$$
 -----(11)

The P.P represents the principle part. The open channels in the <sup>1</sup>p subspace thus make a negative imaginary contribution to W<sub>QQ</sub> which results in singularities in the wave vector in the lower half of the complex E -plane. Equation (9) can be solve to obtained <sup>1</sup>Q subspace component of the wave vector as

$$Q\Psi_C = \frac{1}{E - H_{QQ} - W_{QQ}} V_{QP} \Phi_C^{(+)}$$

Which permits the expression of the P-subspace component of the wave equation as:

$$P\Psi_C = \Phi_C^{(+)} \frac{1}{E^{(+)} - H_{PP}} V_{PQ} \frac{1}{E - H_{QQ} - W_{QQ}} V_{QP} \Phi_C^{(+)}$$

Several factors simplify the description of low energy neutron scattering. The centripetal barrier (columb force) keeps all but l = 0 S wave contribution effectively out of reach of the nuclear interaction for energy greater than 50kev.

The prompt component of the neutron scattering then reduces to S wave elastic scattering in this energy range.

The l = 0 wave function satisfying and incoming waive boundary condition take the form:

$$\Psi_0(r) = i/2 (e^{-ikr} - S_0 e^{ikr}) \quad r \longrightarrow \infty \quad - \quad (13)$$

Where the wave number  $K = 2\sqrt{2\mu E_{cm}} / \hbar$ ,

$\mu$  is the reduced mass and  $E_{cm}$  the centre of mass energy. The wave vector of equation (12) yields an  $l = 0$  S matrix so that can be approximated in the multi-level-Breit-wigner form as:

$$S_{O,ab} = e^{i(\Phi_a + \Phi_b)} \left( \delta_{ab} - i \sum_{\mu} \frac{g_{\mu a} g_{\mu b}}{E - \varepsilon_{\mu} + i\Gamma_{\mu/2}} \right) \dots \dots \dots (14)$$

Where  $\phi_a$  and  $\phi_b$  are the initial and final channel phase shifts and the amplitude  $g_{\mu c}$  characterizes the coupling of compound state  $\mu$  to the channel  $c$  with  $\Gamma_{\mu} = \sum_j g_{\mu c}^2$ .

The first term in this expression is a direct scattering amplitude associated with scattering in the  $^1p$  sub space alone. The second term describes the slower process that result from coupling through the states of the  $^1Q$  subspecies. The first term varies slowly as a function of energy while the second term varies rapidly. (The resonance energy  $\varepsilon_{\mu}$  are not identical to the energy of the compound Nuclear states due to energy shift given by real part of equation (11).

The amplitudes  $g_{\mu c}$  can be positive or negative after extracting an appropriate penetrating factor distributed normally.

Once the S-matrix is known the cross sections can be calculated. For the case of S-wave scattering on a spin zero target, the cross sections directly related to the elastic channel S-matrix element,  $S_{o,aa}$ , are the total, elastic and absorption ones.

$$\sigma_{tot} = \frac{2\pi}{k^2} [1 - \text{Re}^{S_{0,aa}}] \text{-----} \quad (15)$$

$$\sigma_{el} = \frac{\pi}{k^2} |S_{0,aa} - 1|^2$$

Where  $T_0$  is the S-wave transmission coefficient. The reaction cross section and transmission coefficient  $T_0$  are non-zero when the elastic S-matrix element  $S_{0,aa}$  is smaller than one in magnitude., This occur when the flux is pass through a long-lived compound Nucleus states to other channels such as gamma emission or fission.

The cross section takes the form

$$\sigma_{ac} = \frac{\pi}{k^2} |S_{0,aa}|^2$$

One can easily verify that the total flux is conserved.

$$\sigma_{abs} = \sum_{j=1} \sigma_j \text{ and } \sigma_t = \sigma_{elas} + \sigma_{abs}$$

At extremely low energies, below the resonance region the elastic cross section is observed to approach a constant value  $\sigma_{el}^0$ . The value is use to calculate another quantity of physical interest the scattering radius

$$R' = \sqrt{\sigma_{el}^0 / 4\pi}$$

However, only S – wave has been discussed. P-wave resonances are also observed quite frequently (narrow peaks). Even the d-wave resonances are observed in some cases. Due to the centripetal barrier, their partial widths are much smaller than that of the S-wave resonances

### 2.1.4: Optical model

The principle objective of optical model is to describe just the prompt direct reaction in a nuclear collision. To separate the direct reactions from compound – nucleus ones, one assumed that the compound nucleus reaction do not contribute to the average wave function and scattering amplitudes due to their rapid fluctuations in energy. Note that the compound Nucleus reaction still do contribute to the average cross sections which are for the most part, proportional to the squares of the amplitudes. The energy averaged amplitudes however are associated with scattering amplitudes for the prompt components of the scattering. The optical model potential is defined as the potential which furnishes the energy-averaged scattering amplitudes. The use of an effective spherical optical model potential to take into accounts the coupling the excited states of the target as well as being fundamental for the calculation of direct reaction observables. Optical model calculations are also used to produce transmission coefficient essential for the analysis of compound nucleus cross sections with the Hauser-Feshbach statistical theory.

### 2.1.5: Derivation

Returning to the P-subspace wave vector of equation (12) one can write the energy averaged as:

$$\langle P\Psi_i \rangle = \Phi_i^{(+)} + \frac{1}{E^{(+)} - H_{PP}} V_{PQM} \langle 1/e_{QQ} \rangle V_{QP} \text{-----} (16)$$

$$\text{Since } e_{QQ} = E - H_{QQ} - W_{QQ} \text{-----} (17)$$

is the only rapidly varying function of the energy in the expression. The average wave vector can be written in a Schrödinger-equation-like form by multiply both side of the expression in equation (16) by  $E^{(+)} - H_{PP}$ .

$$(E - H_{PP}) \langle P\Psi_i \rangle = V_{PQ} \langle 1/e_{QQ} \rangle V_{QP} \Phi_i^{(+)} \text{-----} (18)$$

Using equation (16) again to rewrite the wave` vector  $\Phi_i^{(+)}$

$$\Phi_i^{(+)} = \frac{1}{1 + (E^{(+)} - H_{PP})^{-1} V_{PQ} (1/e_{QQ}) V_{QP}} \langle P\Psi_i \rangle \text{-----} (19)$$

Substituting this equation (18) and performing a bit of algebra. One finally obtains the optical model equation.

$$E - H_{PP} - V_{PQ} \frac{1}{\langle \frac{1}{e_{QQ}} \rangle^{-1} + W_{QQ}} V_{QP} \langle P\Psi_i \rangle = 0 \text{-----} (20)$$

The optical potential can thus be written as:

$$V_{OPT} = V_{PP} + V_{PQ} \frac{1}{\langle \frac{1}{e_{QQ}} \rangle^{-1} + W_{QQ}} V_{QP} \text{-----} (21)$$

## 2.2 Types of Nuclear Model Codes

**2.2.1: Empire** –II belong to the new generation of statistical model codes. It was officially released in March 1999 (version 2.13 Trieste). Since then, the code has been under constant and intensive development, which leads to significant improvements and extensions. The code is intended as a general theoretical tool to be used in basic research and nuclear data evaluation for calculation of nuclear reactions in the broad range of

incident energies and projectiles. It was designed to contain state of art nuclear reaction modeling, being at the same time very easy to use. A full ENDF-6 formatted file and its graphical comparison with the available experimental data can be obtained with just a few mouse clicks and key strokes. The most recent version EMPIRE-2.16 (Montenotte) includes major nuclear reaction mechanisms, such as optical model (SCAT2), coupled channels (ECIS), Multistep Direct (ORION + TRISTAN), NVWY Multistep Compound, Monte Carlo pre equilibrium emission and the full featured Hauser-Feshbach model with widths fluctuation correction (HRTW). Heavy Ion fission cross section can be calculated within the simplified coupled channels approach (CCFUS). Comprehensive library of input parameters covers nuclear masses, optical model parameters, ground state deformations, discrete levels and decay schemes, level densities, fission barriers (BARFIT), moments of inertia (MOMFIT), and x-ray strength functions. Effects of the dynamic deformation of a fast rotating nucleus can be taken into account in the calculations. The results can be converted into the ENDF-6 format using the accompany code EMPEND by A. Trkov. The package includes the full EXPOR library of experimental data. Relevant EXFOR entries are automatically retrieved during the calculations. By default, plots comparing experimental results with the calculated ones are produced using the extended PLOT4 code linked to the rest of the system through a series of pre-processing codes and bash-shell scripts. Interactive plotting is possible through the powerful ZV Vivew package. Easy operation of the whole system is assumed by the graphic user interface written in Tcl/Tk.

### 2.2.2 Statistical Multi Step Code Exifon

A unique description ( $a, xb$ ) emission spectra where  $a, b = n, p, \alpha$  and  $\gamma$  (Neutron, Proton, Alpha and Gamma-Ray) as well as excitation function (activation cross section) is proposed within a pure statistical multi step reaction model (H. Kalka, 1991). This approach is based on many body theory (Green Function Formalism) (P. Ring and P. Schuck, 1980) and random Matrix Physics (T.A Broody, J. Flores, 1981). The Code 'EXIFON' (Version 2.0) is a generalization of (H. Kalka, 1990) to energies up to 100Mev. It is a fast code which predicts cross section; from one global parameter set. The only adjustable quantity is the pairing shift (Standard Value  $\Delta = 12.8A^{-1/2}$ ). The output of 'EXIFON' can be arranged into END F-6 Format. The following abbreviation are used.

$$\text{Excitation energy } E = E_a + E_b \text{ (composite)}$$

$$\text{Excitation energy } U = E_a + B_a - B_b - E_b \text{ (Residual)}$$

Where  $B_c$  and  $E_c = \hbar Kc / 2\mu$  are the binding and kinetic energies of the ingoing ( $c = a$ ) and outgoing ( $c = b$ ) particles.

### 2.2.3: Activation Cross Section

Model independent relation between optical model and reaction cross section and the energy integrated partial cross section are satisfied at each incident  $E_a$

$$\sigma_a^{(0m)} = \sum_b \sigma_{a,b} \quad (2.2)$$

$$\sigma_{a,b} = \sum_c \sigma_{abc} \quad \text{and} \quad \sigma_{a,,bc} = \sum_d \sigma_{a,bcd}$$

with  $\sigma_{a,b} = \sigma_{a,b}^{SMD} + \sigma_{a,b}^{SMC}$  the total first chance emission. In this context activation cross-section are given by

$$\sigma_{a,b\gamma} = \sigma_{a,b} - \sum_{c \neq \gamma} \sigma_{a,bc} \quad (2.3)$$

$$\sigma_{a,cb\gamma} = \sigma_{a,cb} - \sum_{d \neq \gamma} \sigma_{a,cbd} \quad (2.4)$$

Where  $b, c, d \neq \gamma$ . For example, the  $(n, p)$  – activation cross sections has the form

$$\sigma_{a,p\gamma} = \sigma_{n,p} - \sigma_{n,pn} - \sigma_{n,2p} - \sigma_{n,pa} \quad (2.5)$$

#### 2.2.4: Angular Distributions

Angular distributions are obtained from simple parameterization (Kalbach and Mann, 1981). The double differential emission cross section is given by

$$\rightarrow \frac{d^2 \sigma_{a,xb}(E_a)}{dE_b d\Omega} = \frac{d^2 \sigma_{a,xb}(E_a)}{dE_b} \sum_{L=0}^{L_{\max}} \frac{2L+1}{4\pi} F_L^{(a,xb)}(E_a, E_b) P_L(\cos\theta) \quad (2.6)$$

$$\text{with } F_L^{(a,xb)}(E_a, E_b) = \left[ \frac{d^2 \sigma_{a,xb}[E_a]}{d[E_b]} \right]^{-1} \times \left[ \frac{d\sigma_{a,b}^{SMD}[E_a]}{dE_b} + C_L \frac{d\sigma_{a,b}^{SMC} E_a}{dE} \right]_{a_L[E_b]} \quad (2.7)$$

Where

$$\rightarrow F_0^{(a,xb)} = 1. \text{ Here, for SMC a symmetric } [C_L = 0(1) \text{ for even (odd)}]$$

and MPE an isotropic angular distribution is assumed. (2.8)

The coefficients are taken from (H. Kalka *et al*) for  $[E_a < 25_{\text{Mev}}]$  and for  $E_a \geq 25_{\text{Mev}}$ . The sum in (2.6) is limited to  $L_{\max} = 4$ .

### 2.2.5: The Statistical Multistep Direct (SMD) Cross Section

The SMD cross section is given by

$$\frac{d\sigma_{a,b}^{SMD}(E_a)}{dE_b} = \sum_{x=1}^{(s)} \frac{d\sigma_{a,b}^{(s)}(E_a)}{dE_b} \quad (2.9)$$

Where the cross section, SMD is a sum of the following contributions denoted according to three sequences of exciton and phonon excitations, *i.e.* [ $e_x$ ], [Vib],[ $2e_x$ ], [ $e_x$ , Vib], [vib ,  $e_x$ ] , [2Vib], [ $3e_x$ ],[ $4e_x$ ] and [ $5e_x$ ]. For  $S \geq 3$ , phonon excitations are neglected, since they proved to be negligible.

### 2.2.6: Statistical Multistep Compound (SMC) Cross Section (Basic Formula)

The SMC Cross Section has the familiar form ( $b = n, p, \alpha, \gamma$ ).

$$\frac{d\sigma_{a,b}^{SMC}(E_a)}{E_b} = \sigma_a^{SMC}(E_b) \sum_{N=N_0}^{N_1} \frac{\tau_N(E)}{\hbar} \sum_{\Delta=N} \Gamma_{N,b}^{(\Delta N)}(E, E_b) \uparrow \quad 2.10$$

Where  $\tau_N(E)$  satisfies the time integrated master equation. For each exciton number  $N = N_p + N_h$

### 2.2.7: Statistical Multistep Compound (SMC) Formation Cross – Section

The SMC Formation cross section is defined by

$$\sigma_a^{SMC}(E_a) = \sigma_a^{(om)}(E_a) - \sum_c \sigma_{a,c}^{SMD}(E_a) \quad (2.11)$$

### 2.5.7: Multiple Particles Emission (MPE)

The (MPE) are calculated in the pure SMC concept. For second chance processes ( $a, cb$ ) and  $c \neq \gamma$  we have

$$\frac{d\sigma_{acb}(E_a)}{dE_b} = \int dE_c \frac{d\sigma_{a,c}(E_a)}{dE_c} \sum_{N=N_0}^{N_1} \frac{\tau_{N-1} E_1}{\hbar} \sum_{\Delta N} \Gamma_{N-1,b}^{(\Delta N)}(E_1, E_b) \uparrow \quad (2.12)$$

Here, the equation has to be solved for each intermediate excitation energy.

$$E_1 = E - B_c - E_c$$

The escape widths are calculated using residual excitation energy

$$U = E_1 - E_b - B_b$$

### **2.3 NUCLEAR DATA TYPES AND DATA CENTERS**

The application of nuclear data include all areas of nuclear science and technology , covering energy applications (fission reactor design; nuclear fuel cycles, nuclear safety; reactor monitoring and influence determination; waste disposal and transmutation; accelerator driven systems; fusion device design and plasma processing technologies) as well as non-energy applications cancer radiotherapy; production of radioisotopes for medical and industrial applications; personnel dosimetry and radiation safety; nuclear safeguards; materials analysis and process control; radiation damage studies; detection of concealed explosives and illegal drugs; exploration for oil and other minerals) and basic research (e.g. nuclear astrophysics) and education.

#### **2.3.1: The role of the IAEA nuclear data section**

The nuclear data section (NDS) of the International Atomic Energy Agency (IAEA) carries out the IAEA activities concerning development and dissemination of nuclear and atomic data for applications. In addition, the NDS is involved in technology transfer activities to assist scientists in developing countries.

#### **2.3.2: Nuclear data types**

Nuclear data are commonly categorized in two main groups; nuclear reactions data, describing the interactions of various projectiles such as neutrons, protons or photons

with target nuclei, and nuclear structure and decay data, describing nuclear levels, half-lives and radioactive decay radiations. For both groups, the type of information given can be experimental given can be experimental data or evaluated data (both numeric) or bibliographic.

#### **2.3.4 Bibliographic Data**

References with some description of contents, but no numerical data. Examples are CINDA (Computer Index or Neutron Data) and NSR (Nuclear Science References).

#### **2.3.5 Experimental Data**

Results of individual measurements as reported by the authors. The most important example is EXFOR/CSISRS, the library for experimental nuclear reaction data.

#### **2.3.6 Evaluated Data**

Libraries contain recommended data based on all data available from experiments and/or theory, arrived at after critical analysis of experimental data and their uncertainties, inter and extrapolation, and/or nuclear model calculations. They are stored in strictly defined formats such as ENDF-6 (The international format for evaluated nuclear reaction data) or ENSDF (the format of the evaluated Nuclear Structure data file). The main cross section libraries in ENDF format usually also contain the relevant decay data needed in the main applications.

Nuclear Reaction Data include cross sections, angular and energy distributions of secondary particles, resonance parameters, and related quantities. For neutron induced reactions up to 20 MeV, the libraries are very complete; the coverage for higher energies

is less complete but improving. Experimental data are found in EXFOR, the related bibliography in CINDA; several evaluated data libraries exist up to 20 MeV or higher. For charged-particle induced and photonuclear reactions, selected experimental data are compiled in EXFOR and only few evaluations exist. Heavy-ion data are partly compiled in EXFOR.

**Web address**

**<http://www-nds.iaea.or.at>**

**<http://www.nndc.bnl.gov>**

**<http://www.near.fr/html/databank/>**

**<http://rndc.ippe.obninsk.ru>**

**<http://depin.npi.msu.su/cdfe/>**

**<http://ie.lbl.gov>**

**2.3.7: DATA ACCESS AND SERVICES**

Distribution via the internet today is the main way of distributing numerical nuclear data and therefore the IAEA Nuclear Data Section is offering a variety of electronic services. At the same time, conventional mail services such as sending customized retrievers or complete libraries on magnetic tape, CD-ROM, diskettes, hardcopy, or by email, are continued for the convenience of users with varying needs and technical infrastructure. Users are kept up to date about new data libraries and other developments through the IAEA's Nuclear Data Newsletter.

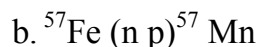
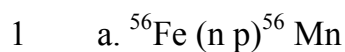
## CHAPTER THREE

### 3.0 MATERIALS AND METHOD

For this research work, the structural materials of the MNSR to be taken into consideration is the beryllium reflector which consist of annular beryllium reflector, top beryllium shim and bottom beryllium reflector. The aim of using beryllium shim is to compensate for fuel burn up, avoid frequent refueling and to reflect fast and slow neutrons. The inner diameter of the annular Be reflector of NIRR-1 is 23.10cm while the outer the diameter of the annular Be-reflector is 43.5cm the height of the annular Be-reflector is 23.85cm and the thickness of the bottom Be-reflector is 5cm (Akaho 2000). For calculation of the excitation function of neutron induced reaction on the structural material of MNSR (NRR1). We consider the different Isotopes of the impurities in the Be reflector based on the percentage abundance. This impurity composition by percentage was obtained from the SAR, 2005:

#### 3.1: The (n.p) Reaction Channel

The cross section of each impurity nuclides with neutron was calculated in (n.p) reaction channel. The outgoing particle in this reaction is charged, occurrence of the reaction depends on the height of coulomb barrier which increases in energy from 1Mev, for  $Z = 3$  to 12Mev for  $Z = 90$ . For impurities in the Be-reflector, the (n.p) reaction cross section was calculated for the following reactions:



- c.  $^{58}\text{Fe} (n p)^{58} \text{Mn}$
- 2) a.  $^{24}\text{Mg} (n p)^{24} \text{Na}$   
 b.  $^{25}\text{Mg} (n p)^{25} \text{Na}$   
 c.  $^{26}\text{Mg} (n p)^{26} \text{Na}$
- 3)  $^{27}\text{Al} (n p)^{27} \text{Mg}$
- 4) a.  $^{28}\text{Si} (n p)^{28} \text{Al}$   
 b.  $^{29}\text{Si} (n p)^{29} \text{Al}$   
 c.  $^{30}\text{Si} (n p)^{30} \text{Al}$
- 5) a.  $^{63}\text{Cu} (n p)^{63} \text{Ni}$   
 b.  $^{65}\text{Cu} (n p)^{65} \text{Ni}$
- 6) a.  $^{14}\text{N} (n p)^{14} \text{C}$   
 b.  $^{15}\text{N} (n p)^{15} \text{C}$
- 7) a.  $^{50}\text{Cr} (n p)^{50} \text{V}$   
 b.  $^{52}\text{Cr} (n p)^{52} \text{V}$   
 c.  $^{53}\text{Cr} (n p)^{53} \text{V}$   
 d.  $^{54}\text{Cr} (n p)^{54} \text{V}$
- 8) a.  $^{64}\text{Zn} (n p)^{64} \text{Cu}$   
 b.  $^{66}\text{Zn} (n p)^{66} \text{Cu}$   
 c.  $^{67}\text{Zn} (n p)^{67} \text{Cu}$   
 d.  $^{68}\text{Zn} (n p)^{68} \text{Cu}$   
 e.  $^{70}\text{Zn} (n p)^{70} \text{Cu}$
- 9) a.  $^{58}\text{Ni} (n p)^{58} \text{Co}$   
 b.  $^{60}\text{Ni} (n p)^{60} \text{Co}$

- c.  $^{61}\text{Ni} (n p)^{61} \text{Co}$
- d.  $^{62}\text{Ni} (n p)^{62} \text{Co}$
- e.  $^{63}\text{Ni} (n p)^{63} \text{Co}$
- 10) a.  $^{204}\text{Pb} (n p)^{204} \text{Ti}$
- b.  $^{206}\text{Pb} (n p)^{206} \text{Ti}$
- c.  $^{207}\text{Pb} (n p)^{207} \text{Ti}$
- d.  $^{208}\text{Pb} (n p)^{208} \text{Ti}$
- 11)  $^{59}\text{Co} (n p)^{59} \text{Fe}$
- 12)  $^{55}\text{Mn} (n p)^{55} \text{Cr}$
- 13) a.  $^{16}_8\text{O} (n p)^{16} \text{N}$
- b.  $^{17}\text{O} (n p)^{17} \text{N}$
- c.  $^{18}\text{O} (n p)^{18} \text{N}$

### 3.2: The (n, $\alpha$ ) Reaction channel

Similarly for the different Isotopes of the impurities in the Be-reflector, the (n,  $\alpha$ ) reaction cross section were calculated,. In this reaction the coulomb barrier is higher than in (n.p) reaction therefore it is not prominent at low energy of neutrons. The coulomb barrier increases with increasing atomic number from 1Mev at  $Z = 2$  to 20Mev at  $Z = 90$ .

This data were calculated for the following reactions:

- a.  $^{54}\text{Fe} (n, \alpha)^{51} \text{Cr}$ ,  $^{56}\text{Fe} (n, \alpha)^{53} \text{Cr}$   $^{57}\text{Fe} (n, \alpha)^{53} \text{Cr}$   $^{58}\text{Fe} (n, \alpha)^{55} \text{Cr}$
- b.  $^{24}\text{Mg} (n, \alpha)^{21} \text{Ne}$ ,  $^{25}\text{Mg} (n, \alpha)^{23} \text{Ne}$   $^{26}\text{Mg} (n, \alpha)^{23} \text{Ne}$
- c.  $^{27}\text{Al} (n, \alpha)^{24} \text{Na}$
- d.  $^{28}\text{Si} (n, \alpha)^{25} \text{Mg}$ ,  $^{29}\text{Si} (n, \alpha)^{26} \text{Mg}$   $^{30}\text{Si} (n, \alpha)^{27} \text{Mg}$

- e.  $^{63}\text{Cu}(n, \alpha)^{60}\text{Co}$ ,  $^{65}\text{Cu}(n, \alpha)^{62}\text{Co}$
- f.  $^{17}\text{N}(n, \alpha)^{11}\text{B}$ ,  $^{15}\text{N}(n, \alpha)^{12}\text{B}$
- g.  $^{50}\text{Cr}(n, \alpha)^{47}\text{Ti}$ ,  $^{52}\text{Cr}(n, \alpha)^{49}\text{Ti}$ ,  $^{53}\text{Cr}(n, \alpha)^{50}\text{Ti}$ ,  $^{54}\text{Cr}(n, \alpha)^{51}\text{Ti}$
- h.  $^{64}\text{Zn}(n, \alpha)^{61}\text{Ni}$ ,  $^{66}\text{Zn}(n, \alpha)^{63}\text{Ni}$ ,  $^{67}\text{Zn}(n, \alpha)^{64}\text{Ni}$ ,  $^{68}\text{Zn}(n, \alpha)^{65}\text{Ni}$ ,  $^{70}\text{Zn}(n, \alpha)^{64}\text{Ni}$
- i.  $^{58}\text{Ni}(n, \alpha)^{55}\text{Fe}$ ,  $^{60}\text{Ni}(n, \alpha)^{57}\text{Fe}$ ,  $^{61}\text{Ni}(n, \alpha)^{58}\text{Fe}$ ,  $^{62}\text{Ni}(n, \alpha)^{59}\text{Fe}$ ,  $^{63}\text{Ni}(n, \alpha)^{60}\text{Fe}$
- j.  $^{204}\text{Pb}(n, \alpha)^{201}\text{Hg}$ ,  $^{206}\text{Pb}(n, \alpha)^{203}\text{Hg}$ ,  $^{207}\text{Pb}(n, \alpha)^{204}\text{Hg}$ ,  $^{208}\text{Pb}(n, \alpha)^{205}\text{Hg}$
- k.  $^{59}\text{Co}(n, \alpha)^{56}\text{Mn}$
- l.  $^{55}\text{Mn}(n, \alpha)^{52}\text{v}$
- m.  $^{16}\text{O}(n, \alpha)^{13}\text{C}$ ,  $^{17}\text{O}(n, \alpha)^{14}\text{C}$ ,  $^{18}\text{O}(n, \alpha)^{15}\text{C}$

### 3.3: Installation and Running of Exifon Code

In this work, the theoretical model code EXIFON which is based on the formalism of optical potential (OM) of the statistical multistep direct (SMD), statistical multistep compound (SMC) and multi particle emission processes (MPE) was used for calculation of excitation function of the neutron induced reaction to the impurities Nuclide in the Be-reflector. The code is a command prompt programme. The excitation functions were calculated from a plot of cross section Vs Energy. The values of the cross section were given in  $10^{-3}$  barns, while that of energies is in MeV. The (n,p) reaction for the various impurity nuclides was considered as (n, p $\gamma$ ) data for comparison with measured cross section data in EXFOR data library. Similarly, the result of (n,  $\alpha$ ) reaction was considered in (n,  $\alpha\gamma$ ) data. Both results were used in plotting a graph of excitation function (a graph of cross section vs Energy).

In order to calculate the excitation function, threshold reaction via (n, p $\gamma$ ) and (n,  $\alpha\gamma$ ) reaction in the energy range of 0 – 20MeV is considered in step of 2MeV at each projectile (neutron) energy.

A simple two body interaction is assumed and a single state particle density of (n, p,  $\alpha$ ) with reduced mass given by:

$$g = 4 \rho (E_F)$$

where the factor 4 takes into cognizance of spin and Isospin degeneracy  $\rho(E_F) = (4.8 \times 10^{-3} \text{Fm}^{-3} \text{MeV}^{3/4}) r_0^{-3} A E^{1/2}$

### 3.3.1: Standard Parameter Set

Other global parameters set for the excitation function are:

- Strength of delta interaction  $F_0 = 27.5 \text{Mev.}$
- Radius Parameter  $r_0 = 1.21 + 4.0A^{-2/3} - 15A^{4/3} \text{Fm}$
- Potential depth  $V_0 = 52.03 \text{Mev.}$
- Fermi Energy  $E_F = 33 \text{Mev.}$
- Paring shift  $A = 12.8A^{-1/2} \text{Mev.}$
- Phonon (Breit – Wigner) width  $\Delta w = 1.4 \text{Mev.}$
- Optical model (Wilmore-Hodgson for Neutron  
Huizenga – Igo, for alphas, Perey et al, for proton)

### 3.3.2: Modifications

In calculation the following parameter can be changed, strength of the residual interaction  $F_0$ , radius parameter  $r_0$ , Fermi energy  $E_f$ , phonon width  $\Delta_w$ , and the global OM parameter set for proton in addition the pairing shifh  $\Delta$  and  $\Delta^{\text{eff}}$  can be modified (also for SMD processes). the pairing energy has the most influence on description of emission spectra especially on activation cross section.

### 3.3.3: Input Data File

Input data file ( i.e. FE56, TA181,PB208, etc.) are necessary for each (target) nucleus. They contain all binding energies  $B_c$  and shell-correction energies  $\delta W$  , as well as phonon parameter  $(\lambda, \omega_\lambda, \beta_\lambda)$  . They can be created (if they do not exist so far) with code INPEXI.EXE. one input data file contain all the information for neutron,proton,and  $\alpha$ - induced reaction.

Reaction channel and arrays

The following reaction channels are considered:

		I=0	I=1	I=2	I=3
SMD	IS=0	(a,n)	(a,p)	(a, $\alpha$ )	(a, $\gamma$ )
SMC	IS=1	(a,n)	(a,p)	(a, $\alpha$ )	(a, $\gamma$ )
SMC	IS=2	(a,nn)	(a,np)	(a,n $\alpha$ )	(a,n $\gamma$ )
SMC	IS=3	(a,pn)	(a,pp)	(a,p $\alpha$ )	(a,p $\gamma$ )
SMC	IS=4	(a, $\alpha$ n)	(a, $\alpha$ p)	(a, $\alpha\alpha$ )	(a, $\alpha\gamma$ )
SMC	IS=5	(a,2nn)	(a,2np)	(a,2n $\alpha$ )	(a,2n $\gamma$ )

For proton-induced the SMC-channel IS=1 split into two components

The following definitions of emission spectra are used:

- Partial first-chance emission: (a,bc)
- Partial second-chance emission: (a,cb)
- Total first-chance emission:  $(a,b) \equiv \sum_c (a,bc)$
- Total emission:  $(a,xb) \equiv (a,b) + \sum_c (a,cb)$

Reaction channels of type (a, $\gamma$ b) are considered.

The following arrays of emission spectra are used:

[K=emission energy point; I=0,1,2,3, particle type (n,p, $\alpha$ , $\gamma$ )]

- SMC(K,I,M)

M=1 first-chance emission (a,b)

M=2 total emission (a,xb)

- SMD (K,I,N)

N=0 total SMD cross section ( $=[\text{ex}]+[\text{vib}]+[2\text{ex}]+\dots$ )

N=1 [ex]

N=2 [vib]

N=3 [2ex]

N=4 [ex,vib]+[vib,ex]

N=5 [2vib]

N=6 [3ex]

N=7 [4ex]

N=8 [5ex]

- SMD (K,3,0)-DSD cross section
- SMC (K,I,1)-total SMC cross section
- SMC (K,I,N)-isospin component of SMC

N= 0 for T

N= 1 for T

- SMC (K,I,IS)-partial second-chance emission

	I=0	I=1	I=2	I=3
IS=2	(a,nn)	(a,np)	(a,n $\alpha$ )	(a,n $\gamma$ )
IS=3	(a,pn)	(a,pp)	(a,p $\alpha$ )	(a,p $\gamma$ )
IS=4	(a, $\alpha$ n)	(a, $\alpha$ p)	(a, $\alpha\alpha$ )	(a, $\alpha\gamma$ )
IS=5	(a,2nn)	(a,2np)	(a,2n $\alpha$ )	(a,2n $\gamma$ )

- SGA (K,I,M)-partial first-chance emission:

	I=0	I=1	I=2
M=0	(a,nn)	(a,pn)	(a, $\alpha$ n)
M=1	(a,np)	(a,pp)	(a, $\alpha$ p)
M=2	(a,n $\alpha$ )	(a,p $\alpha$ )	(a, $\alpha\alpha$ )
M=3	(a,n $\gamma$ )	(a,2p $\gamma$ )	(a, $\alpha\gamma$ )

- **FL(K,I,L)-Legendre coefficient**
- DD(K,I,N)-double – differential cross section of (a,xb) for fixed emission energy of fixed emission angle.

### 3.3.4: Output Data File

The emission spectra of neutron, proton,  $\alpha$ -particle, and photons are stored in the file AXN.DAT,AXP.DAT,AXA.DAT, respectively. They contain the emission energy  $E_b$  and the following 9(nine) reaction channels:

SMG(K,1,2)

SMG(K,I,1)

SMD(K,I,0)

SMD(K,I,1)

SMD(K,I,3)

SMD(K,I,6)

SMD(K,I,7)

SMD(K,I,8)

SMC(K,I,1)

These arrays can be change in subroutine plot.

The activation cross section (a,2n), (a,p), and (a, $\alpha$ ) are stored in A2N.DAT, AP.DAT, and ALF.DAT, respectively. They contain the incident energy  $E_c$  ( in LS) and the arrays: the array can be changed in subroutine EXIFON.

Legendre coefficient for n,pand  $\alpha$ , are stored in LGN.DAT,LGP.DAT,LGA.DAT, respectively. Double-differential cross section are stored in EN...N.DAT,EN...P.DAT,EN...A.DAT ( for fixed emission energy) and in DG...N.DAT,DG...P.DAT and DG...A.DAT ( for fixed emission angle). This array can be changed in subroutine ANG.A,short documentation after each run is written to file OUTEXI.

### **3.4: Exfor Data Library Retrieval**

The EXFOR Data Library is a unified computerized system (Library format) by which International, Regional and National data analysis centers exchange experimental nuclear reaction data. Compilation and exchange of experimental Nuclear reaction data is coordinated by the International Atomic energy Agency (IAEA). The U.S. version of

EXFOR is CSISRS, coverage is complete for neutron data, (in particular up to  $20\text{Mev}$ ) and less complete (but improving) for higher energy neutrons charged particle induced and photonuclear data. In this library there are more than 60,000 data set and more than 3 million data point. Spanning the period of 1978 to 2007 (ICTP 2001).

EXFOR library also contains numerical tables and structured abstract with experimental and bibliographic information. The main users of the EXFOR library are evaluators. (EXFOR data base is starting point for all evaluations) applied users if no evaluation available and those measuring or calculating cross-section data.

### **3.4.1: Access to EXFOR Library**

The EXFOR is available for interactive retrievals through World Wide Web (www) and telnet (one reaction at a time). Also, on two CD-ROM versions (same data base, different retrieval software) both developed by nuclear data library (NDS) of the IAEA complicated retrievals are available individually on request from IAEA –NDS (diskette, tape, file transfers, e-mail, and print out) EXFOR output are in formats and these include standard format (Exchange formats), computational format, for plotting and further processing from the IAEA and online plots for inter comparison with evaluated data “BNL325” “ZV View”.

Finally a plot of both EXFOR and EXIFON results of excitation function will be used for this research work. From which further analysis can be give insight to the suitability of each model.

## CHAPTER FOUR

### 4.0 RESULTS AND DISCUSSION

The theoretical model code EXIFON was used to determine the excitation function of the nuclides of impurities in the Be-reflector of NIRR-1. The theoretical model is based on optical potentials, which comprises of both statistical multistep (SMD), statistical multistep compound (SMC) and multi particle emission (MPE) adequately describes the interaction between neutron and the nuclides of the impurity isotopes in the energy range of 0 – 20MeV. Calculated data were compared with the experimental data from EXFOR Data Library.

The excitation functions showing calculated data and measured data are given below:

#### 4.1. Fe Nuclides

The stable isotopes of Fe are  $^{54}\text{Fe}$ ,  $^{56}\text{Fe}$ ,  $^{57}\text{Fe}$ ,  $^{58}\text{Fe}$ , with the following isotopic abundance  $^{54}\text{Fe}$  (5.845)  $^{56}\text{Fe}$  (91.754)  $^{57}\text{Fe}$  (2.119)  $^{58}\text{Fe}$  (0.282)

The nuclides of  $^{54}\text{Fe}$ ,  $^{56}\text{Fe}$ ,  $^{57}\text{Fe}$ ,  $^{58}\text{Fe}$  with concentration greater than 4000ppm constitute majority of the impurities in Be-reflector. The (n p) reaction channel on  $^{58}\text{Fe}$  does not exist, and accounts for only 0.282% of the isotopic abundance of Fe. However, the isotopic abundance of  $^{56}\text{Fe}$  and  $^{54}\text{Fe}$  are respectively calculated in the (n,p) reaction data on  $^{54}\text{Fe}$ , and  $^{56}\text{Fe}$  and mostly agree well when compared with data from “EXFOR”. However, the experimental data EXFOR were scanty and mostly measurement were made around 14 MeV. Likewise the (n  $\alpha$ ) reaction are scanty and discrepant from the

experimental data and no data was found on  $^{57}\text{Fe}$   $^{58}\text{Fe}$ ; via (n  $\alpha$ ) reaction channel. Only the theoretical model was able to account for the excitation function of both  $^{57}\text{Fe}$  and  $^{58}\text{Fe}$ , while the data retrieved from EXFOR on  $^{54}\text{Fe}$  and  $^{56}\text{Fe}$ , were very few and scanty, mostly are not in good agreement with the theoretical model code EXIFON.

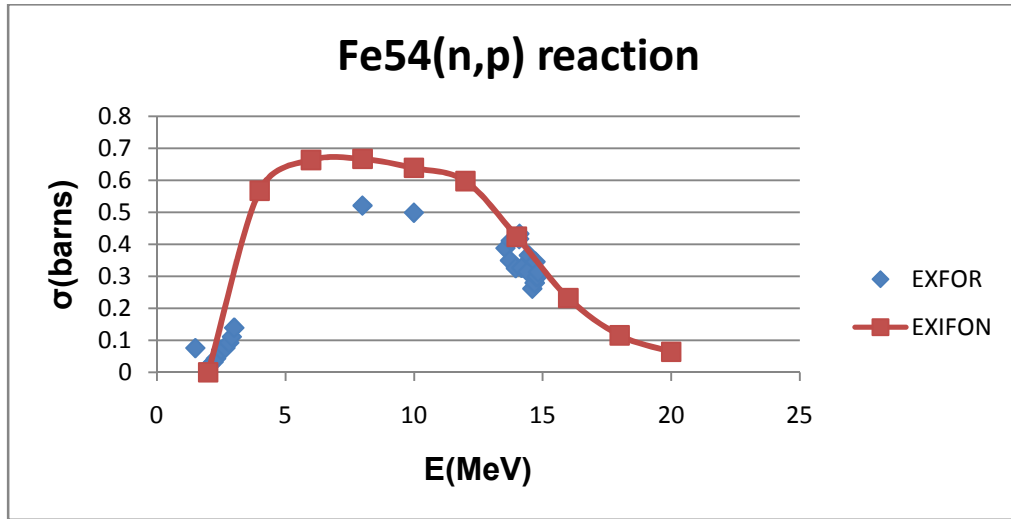


Figure 4.1a

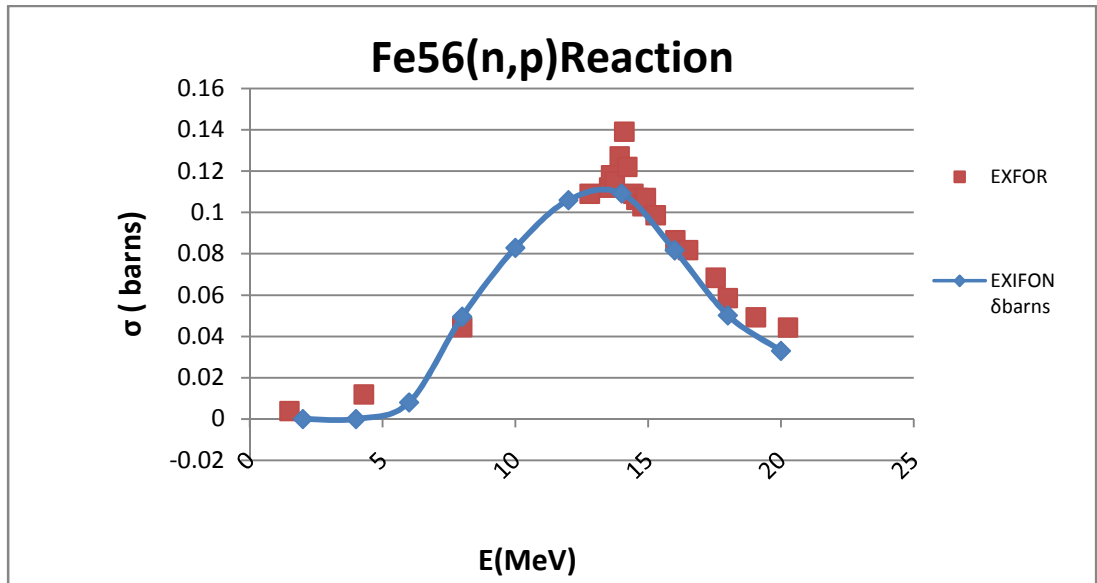


Figure 4.1b

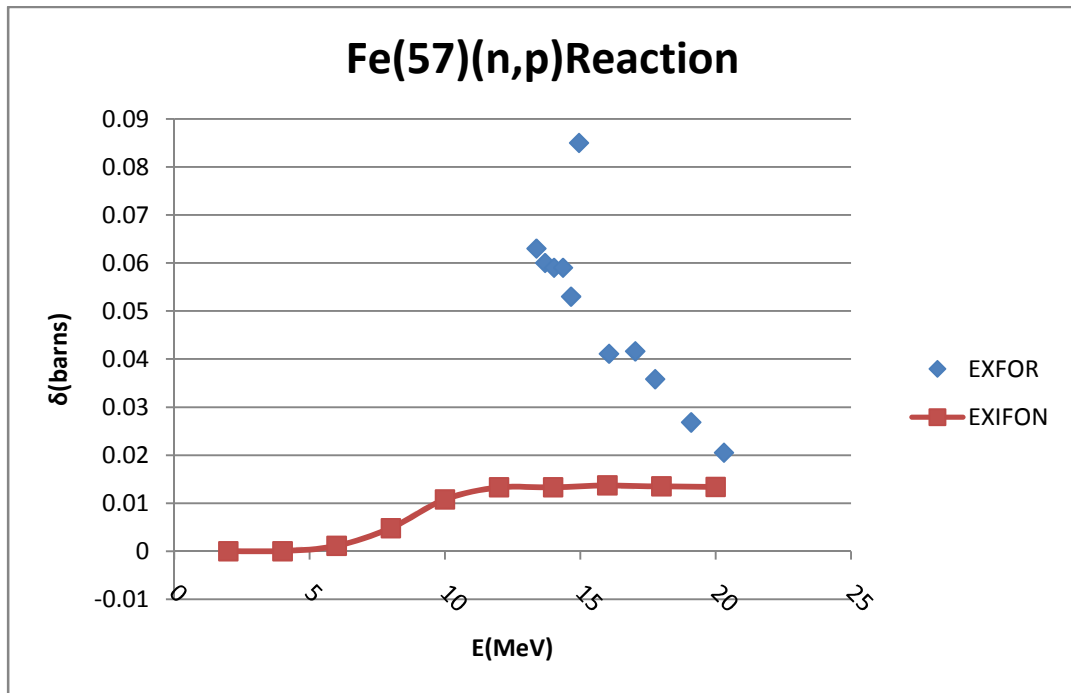


Figure 4.1c

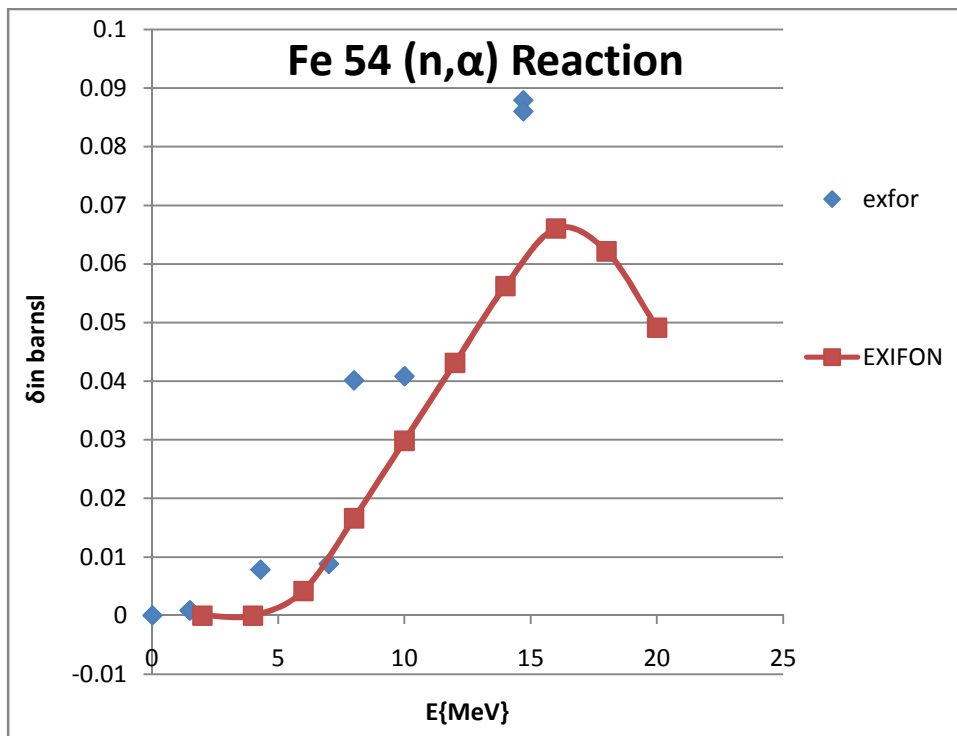


Figure 4.1d

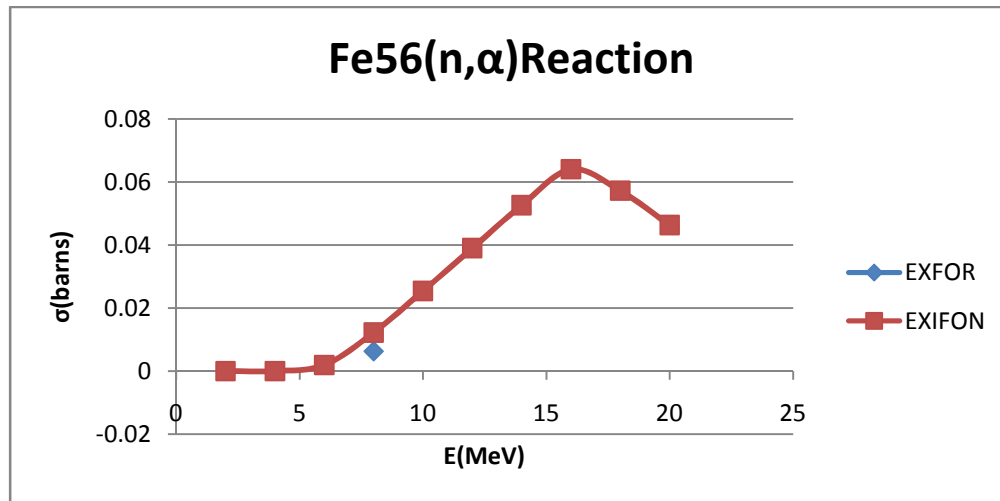


Figure 4.1e

#### 4.2. Al Nuclides

Aluminium has only one stable isotope, i.e.  $^{27}\text{Al}$ , with concentration of 3000ppm, in the Be-reflector of NIRR-1. Therefore, excitation function of Al nuclides are made up of only two measured data from EXFOR data library. Overall, the calculated data are in agreement with theoretical model EXIFON. The measured excitation function in the  $(n,\alpha)$  reaction channel are very few and scanty but are in good agreement with the theoretical models code EXIFON

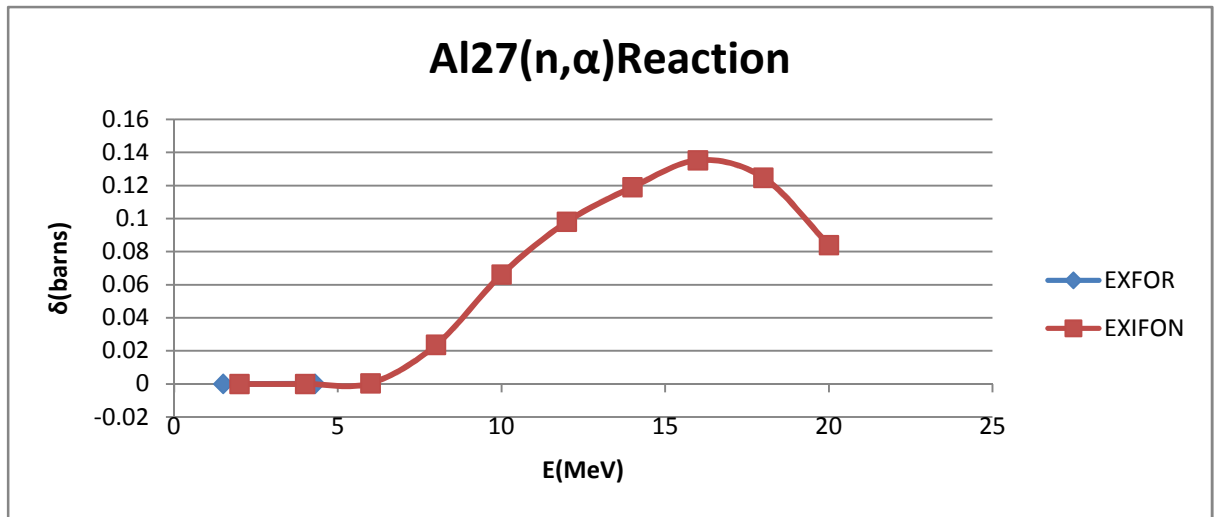


Figure 4.2a

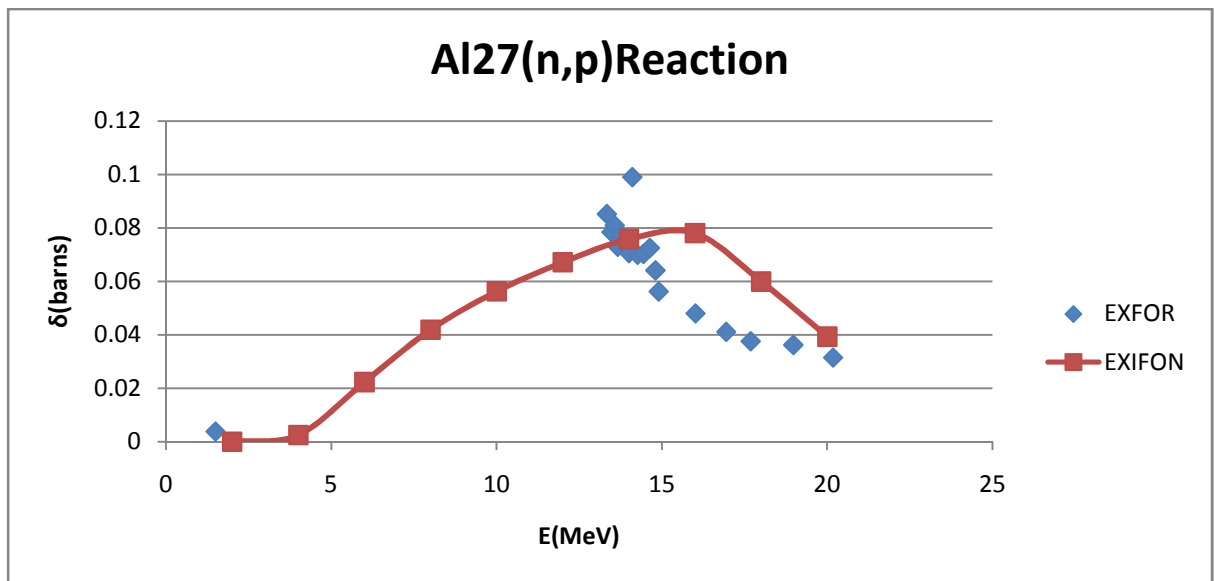


Figure 4.2b

### 4.3. Si Nuclides

The stable isotopes of Si are  $^{28}\text{Si}$   $^{29}\text{Si}$   $^{30}\text{Si}$ , with the following isotopic abundance  $^{28}\text{Si}$  (92.230)  $^{29}\text{Si}$  (4.683)  $^{30}\text{Si}$  (3.087). The (n p) reaction channel for  $^{28}\text{Si}$  and  $^{29}\text{Si}$  were calculated. No data was measured data was obtained for  $^{29}\text{Si}$  from the theoretical code

EXIFON. There is a good agreement between theoretical code and measured data especially for data measured around 13.4MeV to 20.3MeV in the case of  $^{28}\text{Si}$ . While for  $^{30}\text{Si}$  only one data was retrieved from measured data. The (n  $\alpha$ ) reactions for suitable nuclides of Si, no data were found on EXFOR on both  $^{28}\text{Si}$  and  $^{29}\text{Si}$ . But for  $^{30}\text{Si}$  the (n  $\alpha$ ) reaction shows a good agreement between EXIFON and measured data.

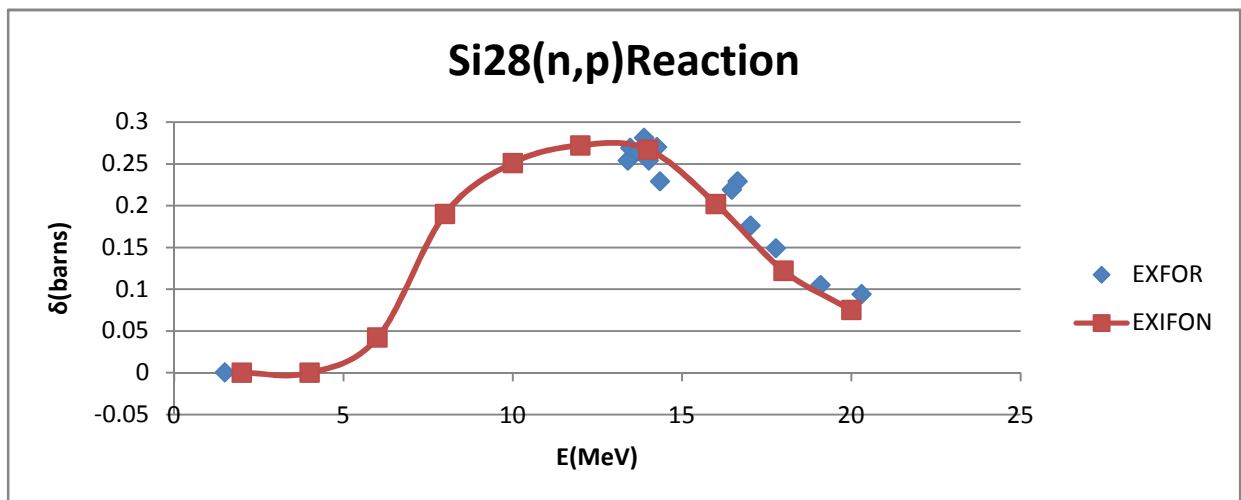


Fig. 4.3a

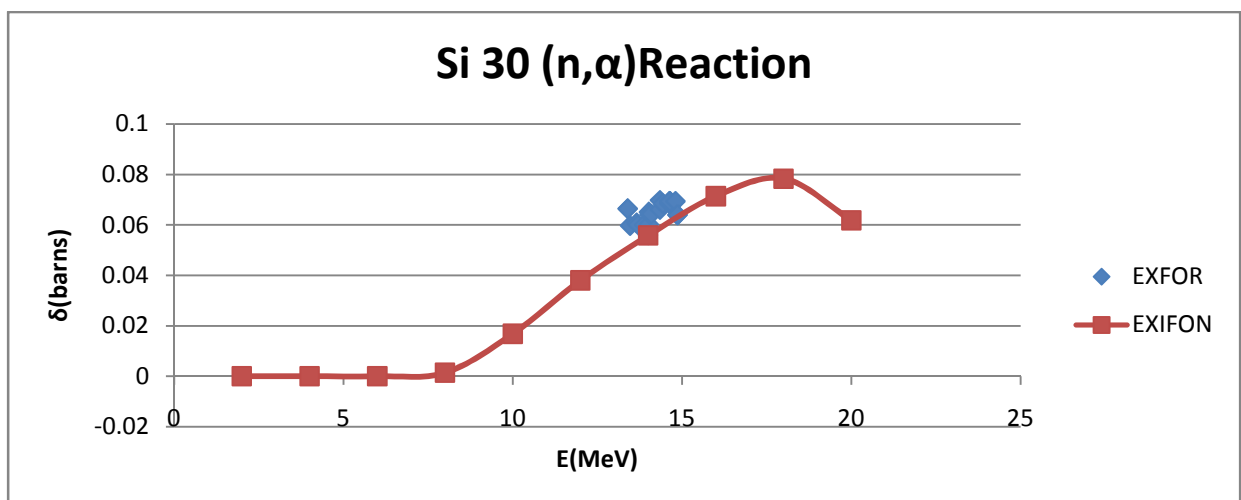


Fig. 4.3a

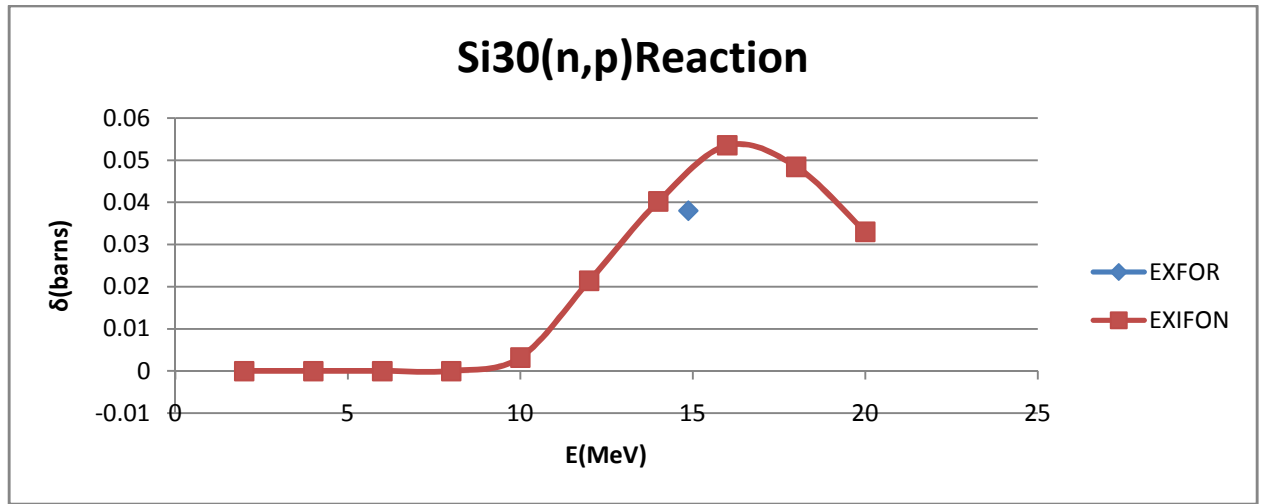


Fig. 4.3c

#### 4.4. Cu Nuclides

The stable isotopes of Cu are  $^{63}\text{Cu}$  and  $^{65}\text{Cu}$ . The (n,p) reaction channel shows good agreement between EXIFON and measured data for  $^{65}\text{Cu}$ , especially around 13.56 – 14.78 MeV. While for  $^{63}\text{Cu}$  (n,p) reaction data does not exist on measured data. In the case of (n,  $\alpha$ ) reaction channel result of excitation functions of nuclide of  $^{63}\text{Cu}$  and  $^{65}\text{Cu}$  both exist and are in good agreement especially around 0 – 14 MeV.

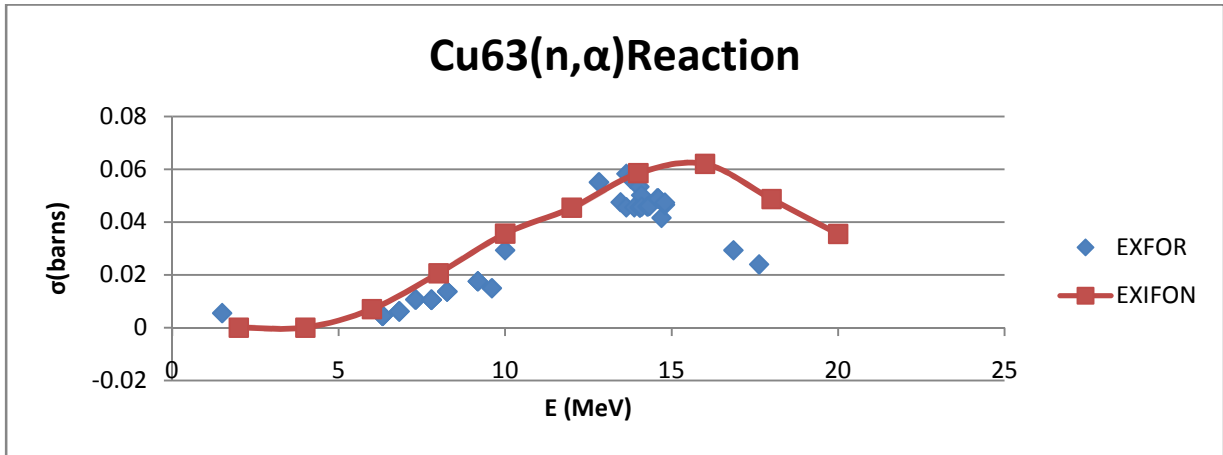


Fig. 4.4a

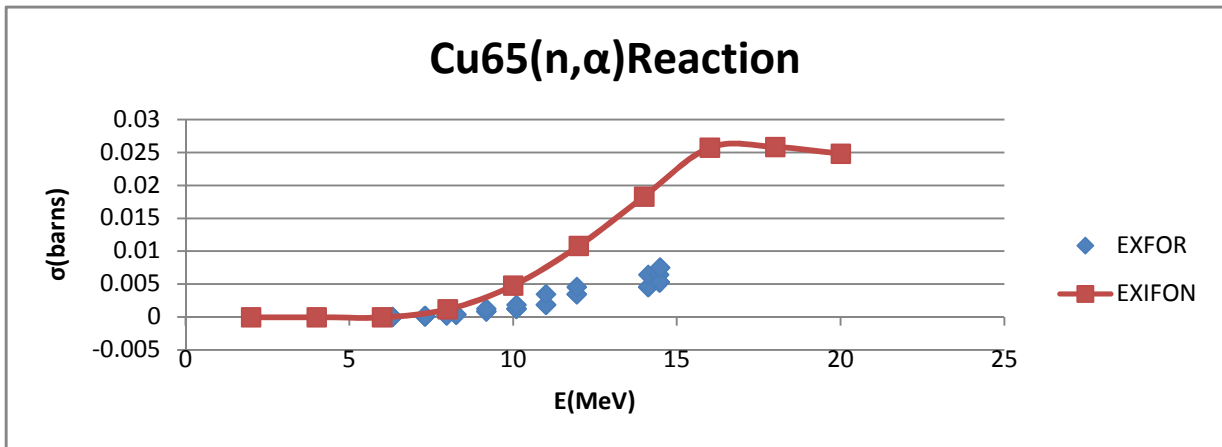


Fig. 4.4b

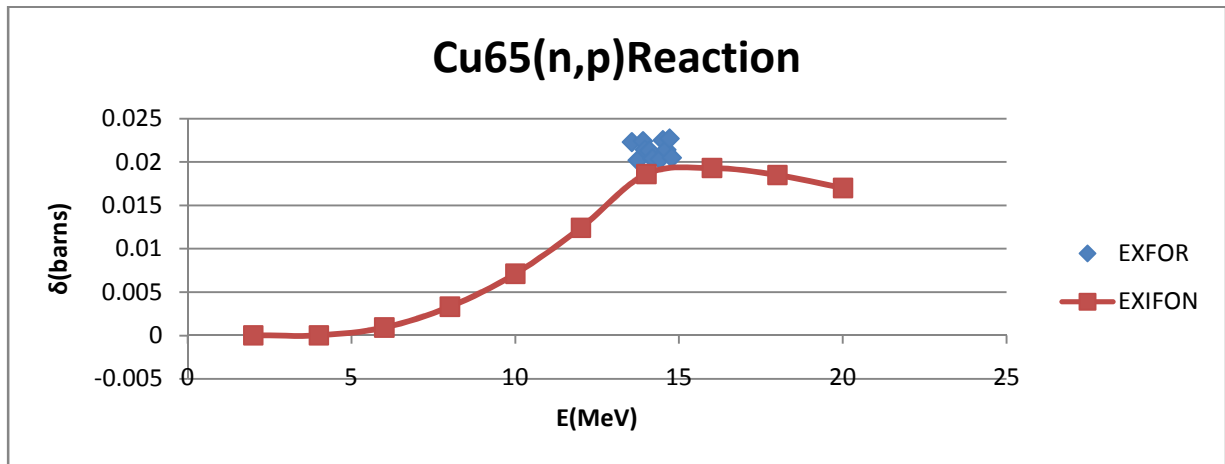


Fig. 4.4c

#### 4.5. N Nuclides

The stable isotopes of N are  $^{14}\text{N}$  and  $^{15}\text{N}$  Nuclides with concentration of 200ppm as part of the impurities on Be reflector, the (n, p) reaction for  $^{15}\text{N}$  does not exist on the EXIFON code which account for only 0.366% of the abundance Nitrogen isotope. Both  $^{14}\text{N}$  which account for 99.634%, the cross section of (n,p) reaction retrieve from EXFOR were incomplete and only at a range of 0 – 1MeV.

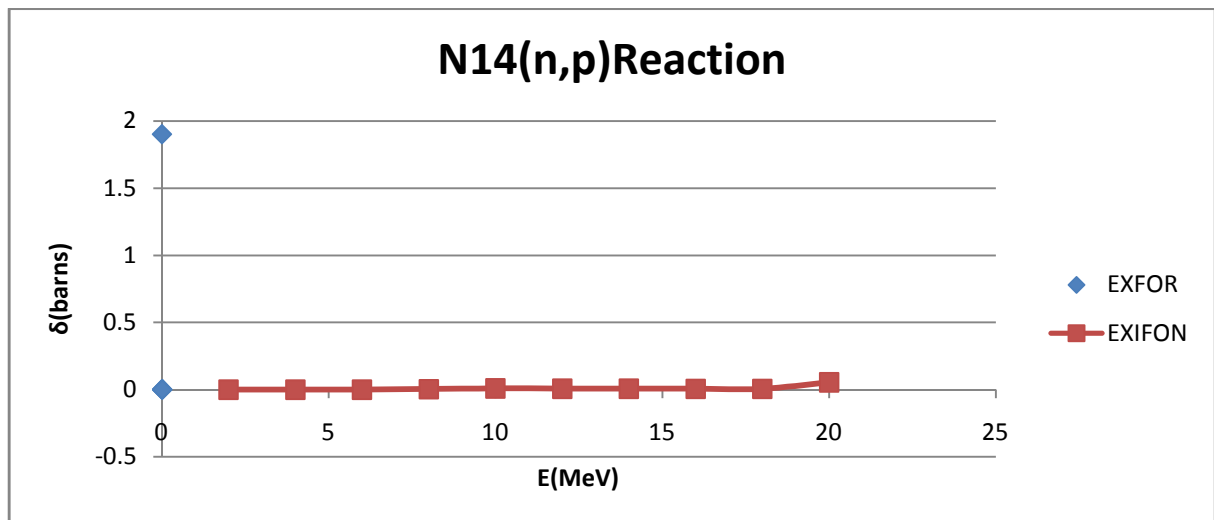


Fig. 4.5a

#### 4.6. Cr Nuclides

The stable isotopes of Cr are  $^{50}\text{Cr}$ ,  $^{52}\text{Cr}$ ,  $^{53}\text{Cr}$ ,  $^{54}\text{Cr}$ . The (n, p) reaction channels for  $^{52}\text{Cr}$  which account for 83.78% of the isotopic abundance compares well between EXIFON and measured data. While there was complete disagreement for  $^{53}\text{Cr}$  between EXIFON and measured data. Again there was no data for  $^{50}\text{Cr}$  and  $^{54}\text{Cr}$  from measured data. While for (n  $\alpha$ ) reaction no data was found on  $^{50}\text{Cr}$ ,  $^{52}\text{Cr}$ ,  $^{53}\text{Cr}$ , except for  $^{54}\text{Cr}$ , which shows complete disagreement between EXIFON and measured data

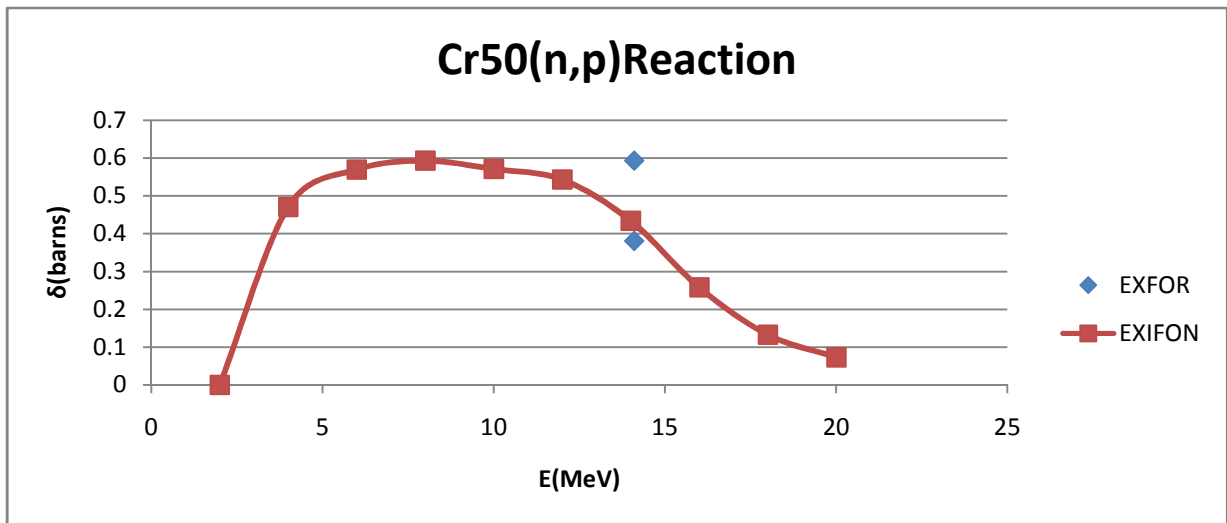


Fig. 4.6a

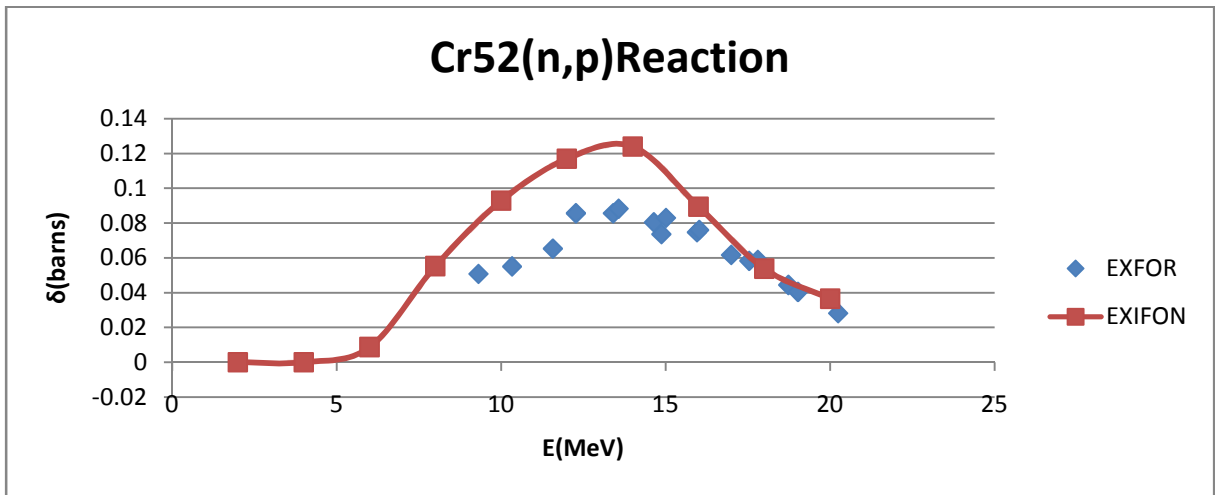


Fig. 4.6b

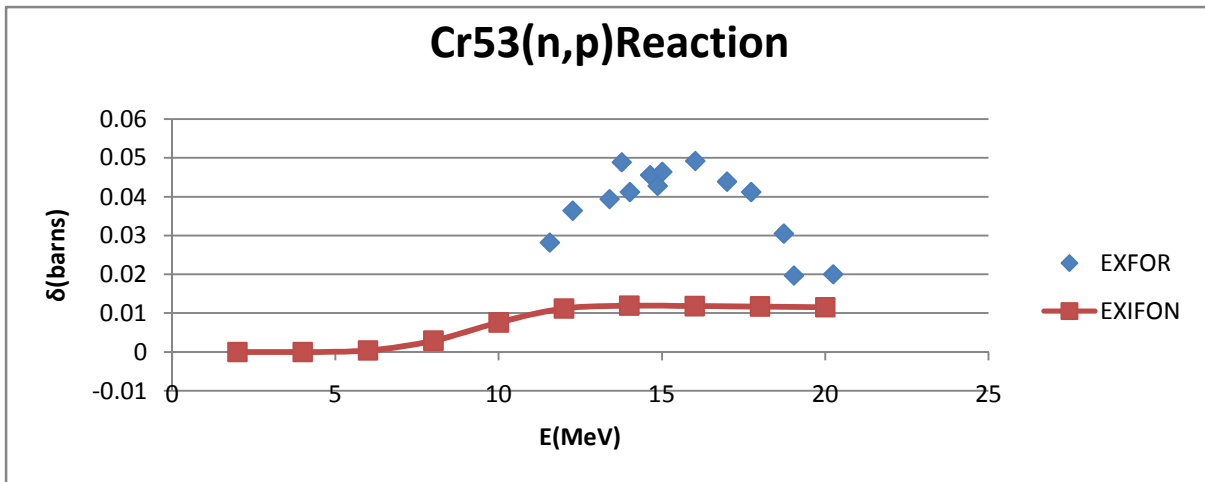


Fig. 4.6c

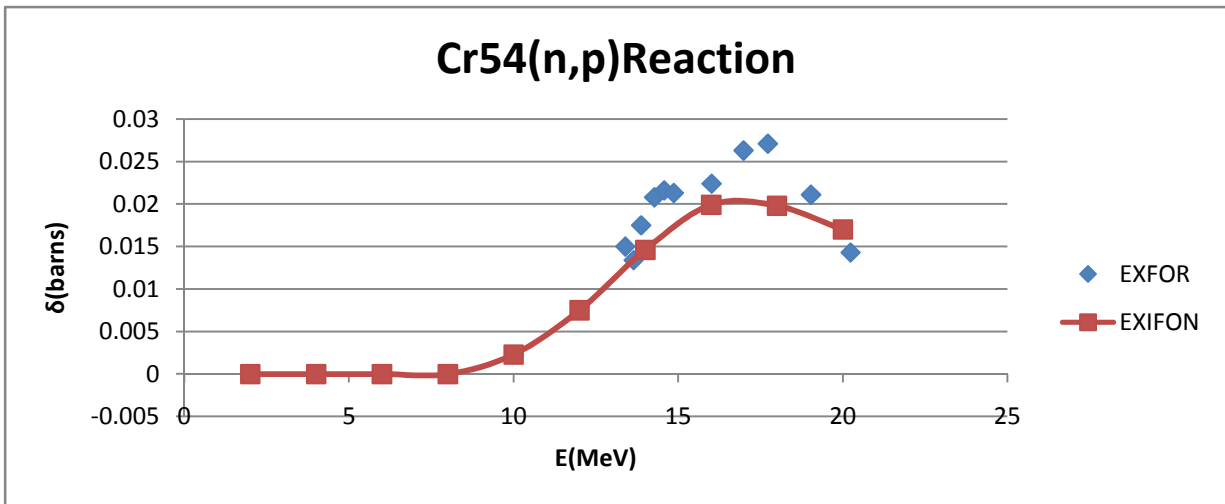


Fig. 4.6d

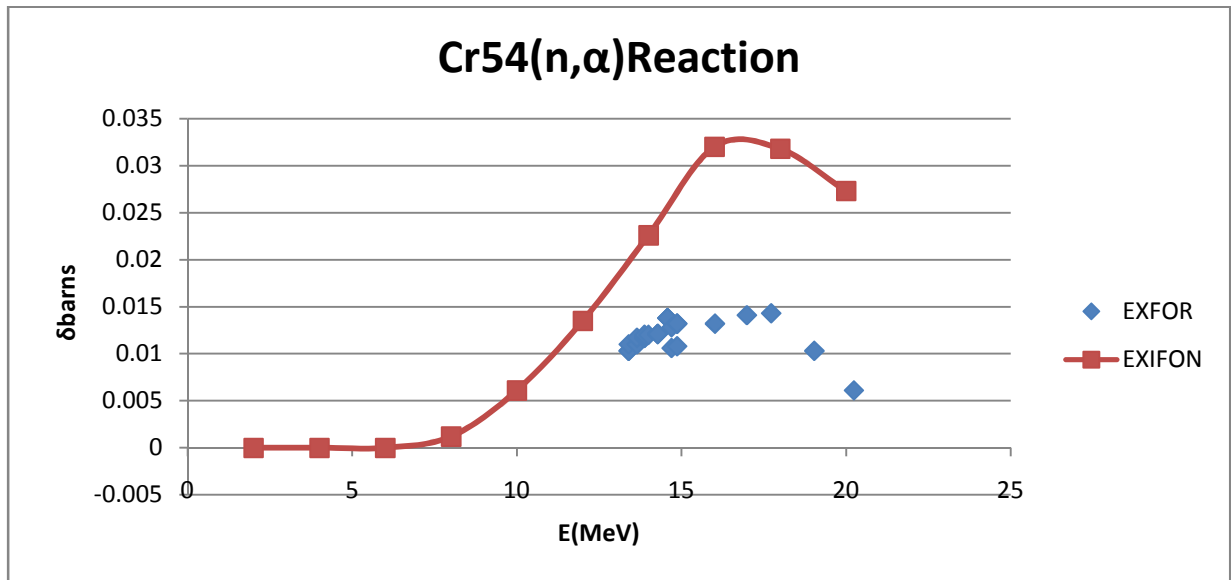


Fig. 4.6e

#### 4.7. Zn Nuclides

Stable isotopes of Zn are  $^{64}\text{Zn}$ ,  $^{66}\text{Zn}$ ,  $^{67}\text{Zn}$ ,  $^{68}\text{Zn}$ ,  $^{70}\text{Zn}$  with the isotopic abundance  $^{64}\text{Zn}$  (48.63)  $^{66}\text{Zn}$  (27.90)  $^{67}\text{Zn}$  (4.10)  $^{68}\text{Zn}$  (18.75)  $^{70}\text{Zn}$  (0.62). The (n p) reaction channel from both EXIFOR and measured data mostly disagree with the exception of  $^{70}\text{Zn}$  and  $^{67}\text{Zn}$ , which have no data on the experimental data library. While for (n α) reactions channel, no data was found for  $^{66}\text{Zn}$  and  $^{67}\text{Zn}$  on measured data.

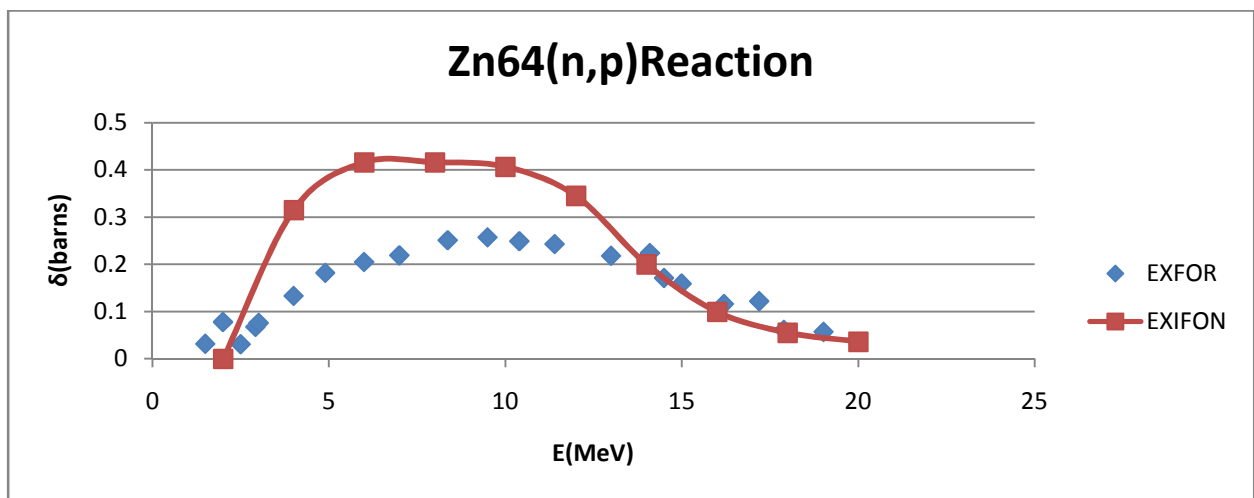


Fig. 4.7

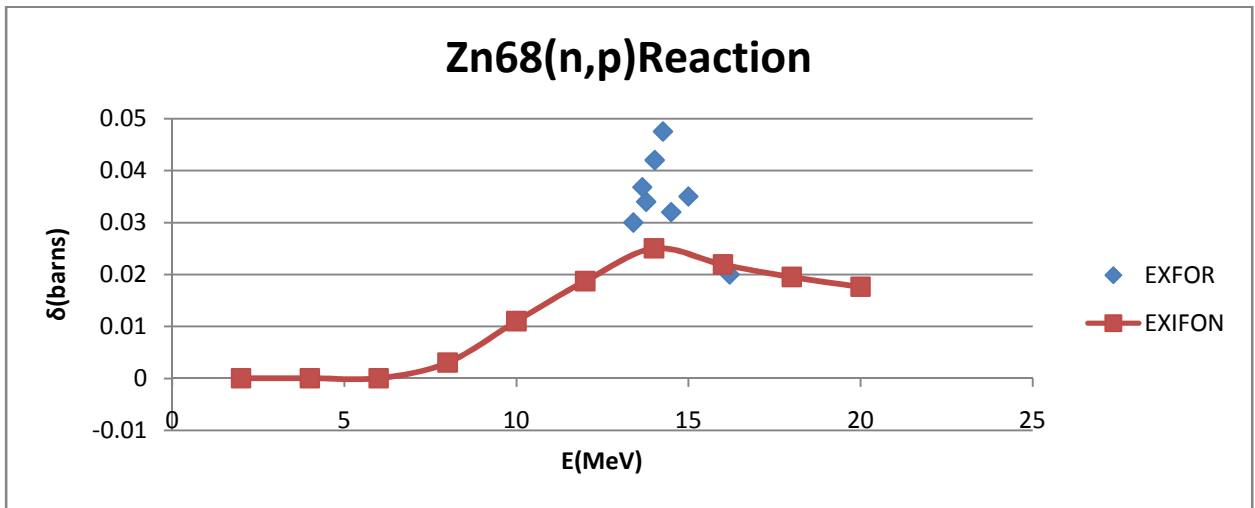


Fig. 4.7b

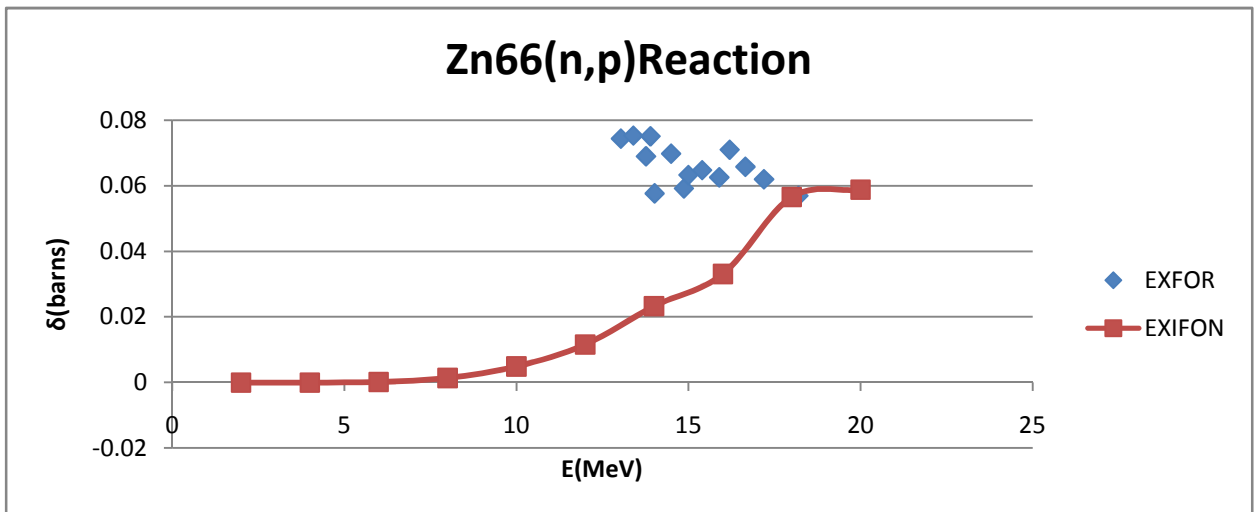


Fig. 4.7c

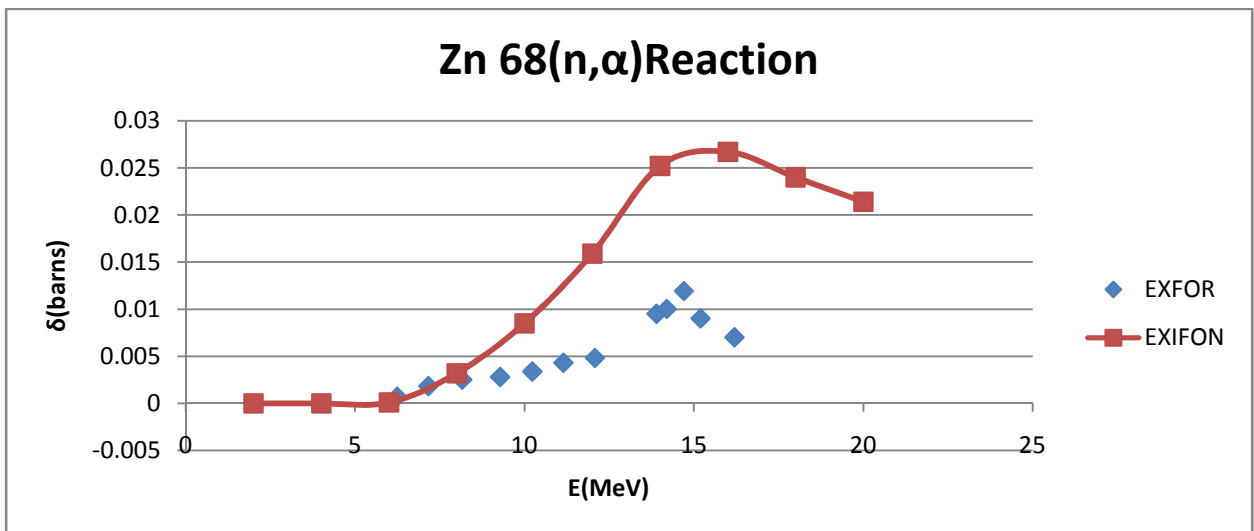
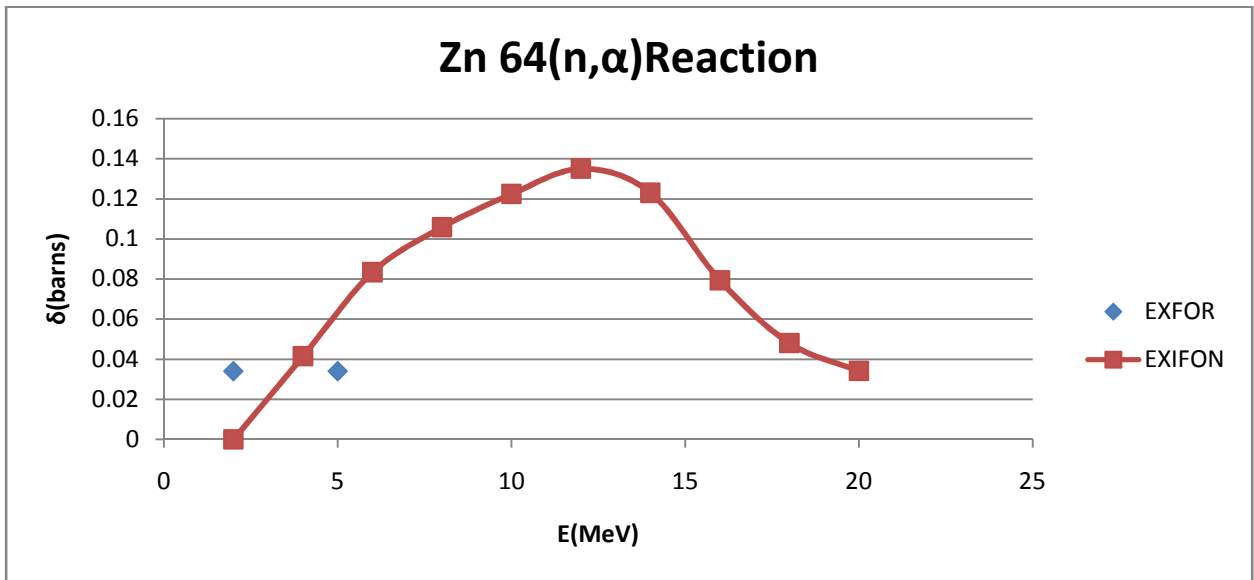


Fig. 4.7c

#### 4.8. Ni Nuclides.

The stable isotopes of Ni are  $^{58}\text{Ni}$ ,  $^{60}\text{Ni}$ ,  $^{61}\text{Ni}$ ,  $^{62}\text{Ni}$ ,  $^{63}\text{Ni}$  with isotopic abundance  $^{58}\text{Ni}$  (68.077)  $^{60}\text{Ni}$  (26.223)  $^{61}\text{Ni}$  (1.140)  $^{62}\text{Ni}$  (3.634)  $^{63}\text{Ni}$  (0.926). The best result was obtained from  $^{58}\text{Ni}$  nuclide, both (n p) and (n  $\alpha$ ) reaction agrees well for EXIFON and experimental data. Likewise there is also a good agreement in the plots measured data

and EXIFON for  $^{60}\text{Ni}$  nuclide (n, p) reaction, but in the case of  $^{61}\text{Ni}$  (n p) reaction there was no agreement. The (n  $\alpha$ ) reaction channel for  $^{60}\text{Ni}$ ,  $^{61}\text{Ni}$  does not exist on measured data library, only that of  $^{62}\text{Ni}$  nuclide, which shows agreement between EXIFON and measured data.

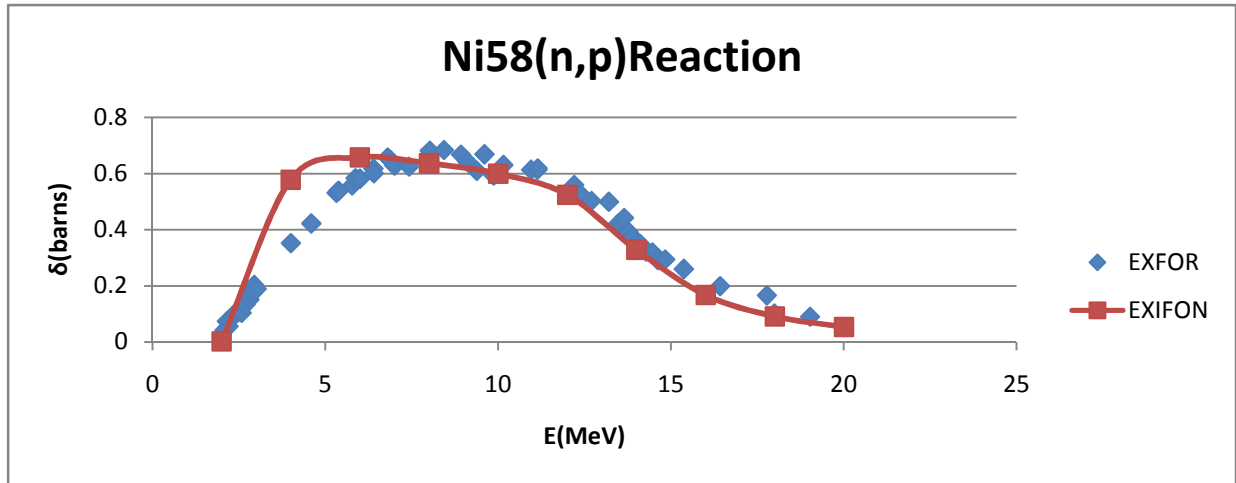


Fig. 4.8a

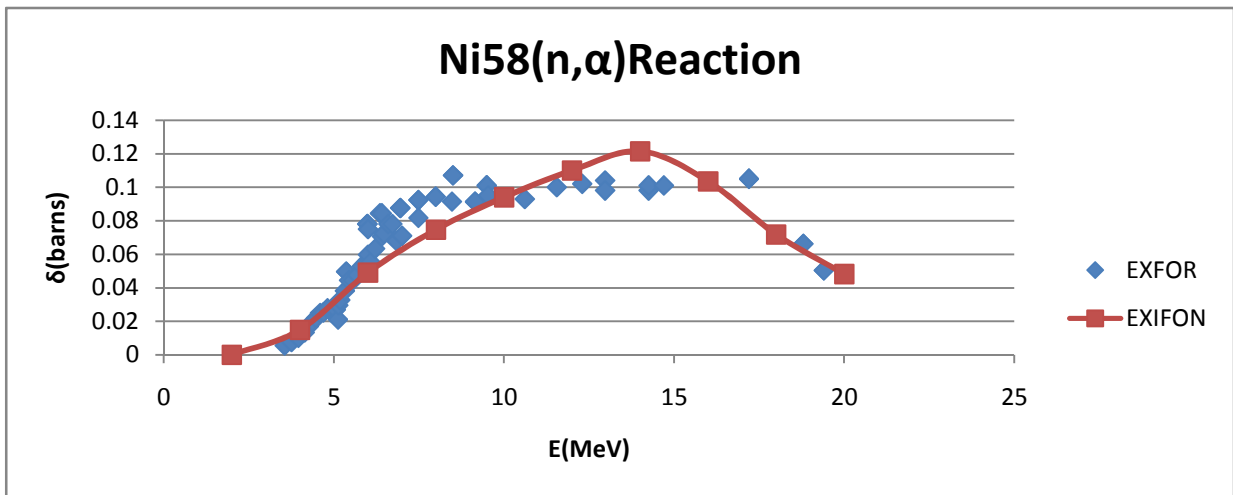


Fig. 4.8b

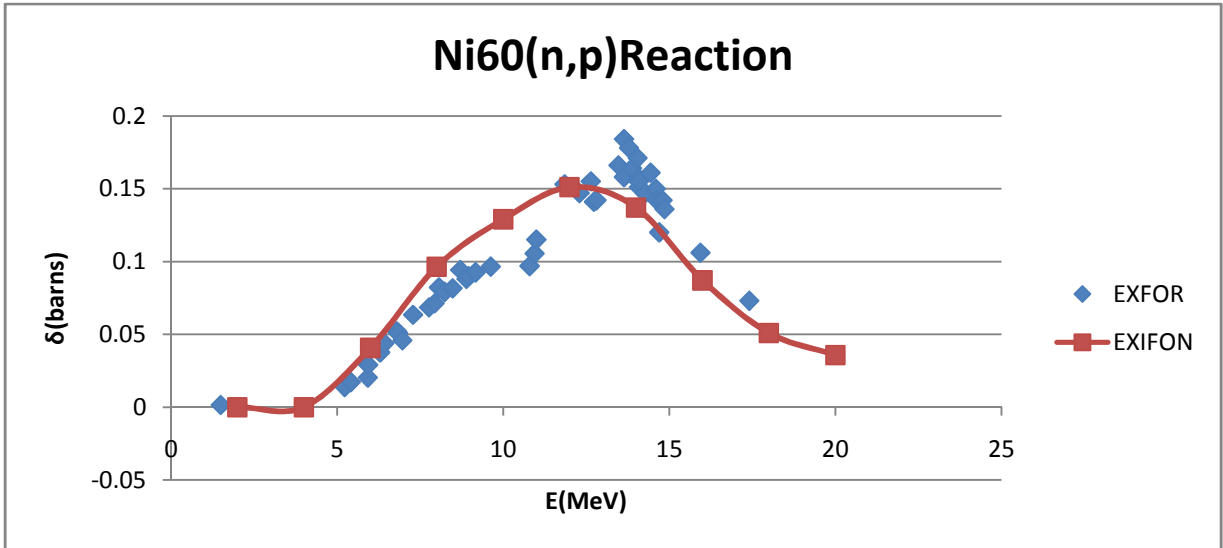


Fig. 4.8c

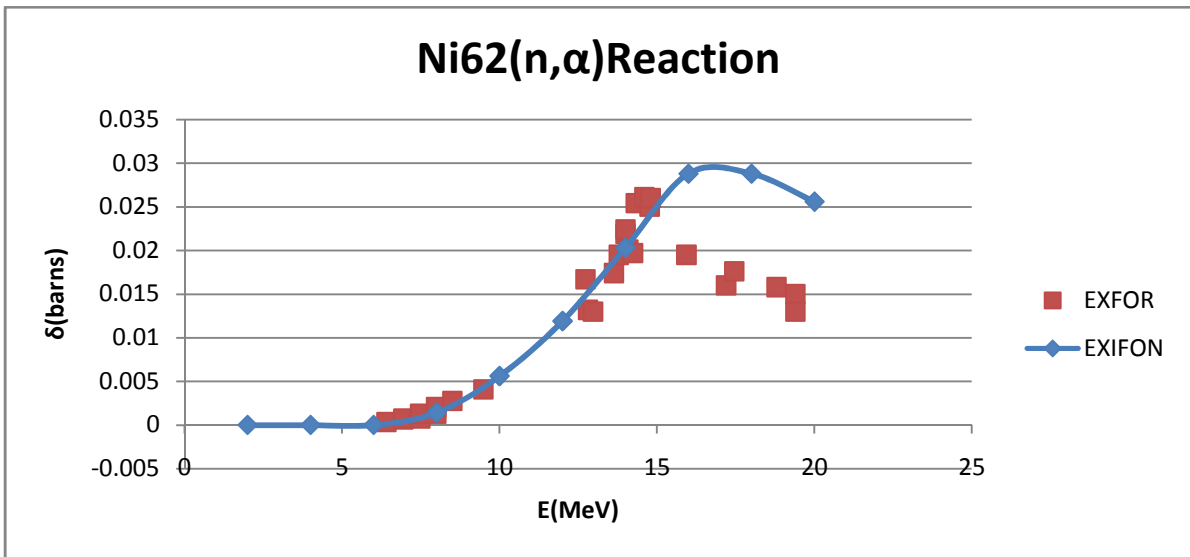


Fig. 4.8d

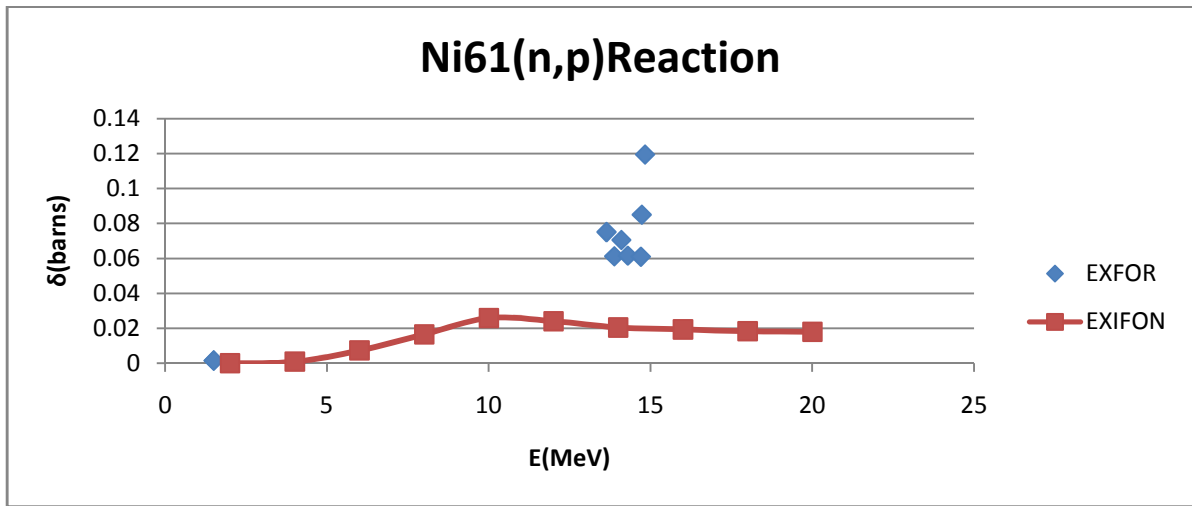


Fig. 4.8d

#### 4.9. Pb Nuclides

The stable isotopes of Pb are  $^{204}\text{Pb}$ ,  $^{206}\text{Pb}$ ,  $^{207}\text{Pb}$  with isotopic abundance  $^{204}\text{Pb}$  (1.4)  $^{206}\text{Pb}$  (24.1)  $^{207}\text{Pb}$  (22.1)  $^{208}\text{Pb}$  (52.4). The  $^{208}\text{Pb}$  Nuclide (n p) reaction channel shows a very good agreement between EXIFON and measured data which account for 52.4% of the isotopic abundance, while no data was found for  $^{204}\text{Pb}$ ,  $^{206}\text{Pb}$ ,  $^{207}\text{Pb}$ . Similarly (n  $\alpha$ ) reaction for  $^{206}\text{Pb}$  good agreement between EXIFON and measured data especially in the energy range of 13-20MeV, while no data was obtained for  $^{204}\text{Pb}$ ,  $^{207}\text{Pb}$  and  $^{208}\text{Pb}$  in measured data.

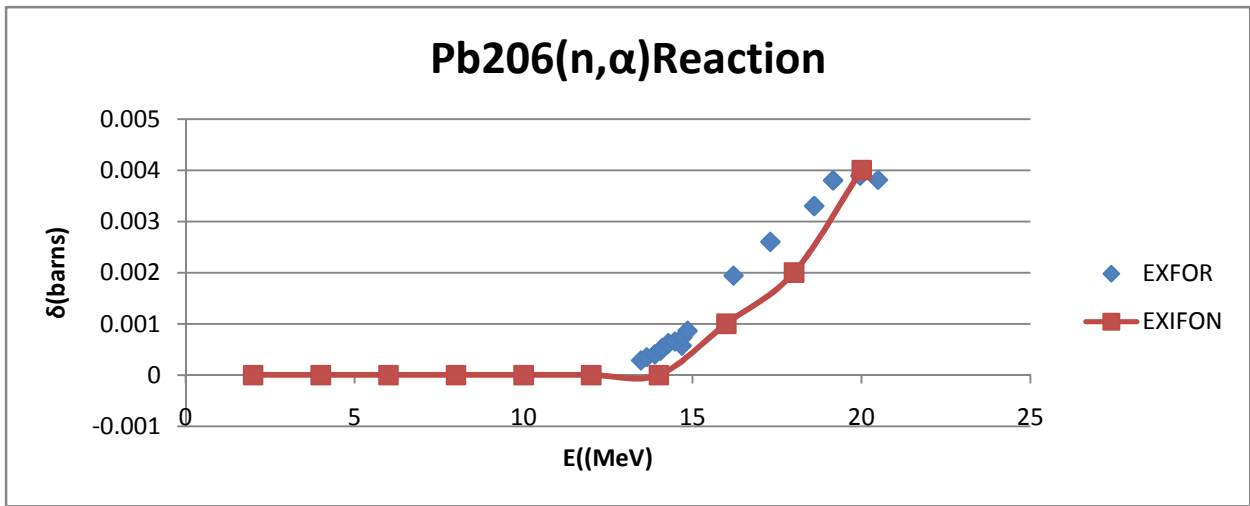


Fig. 4.9a

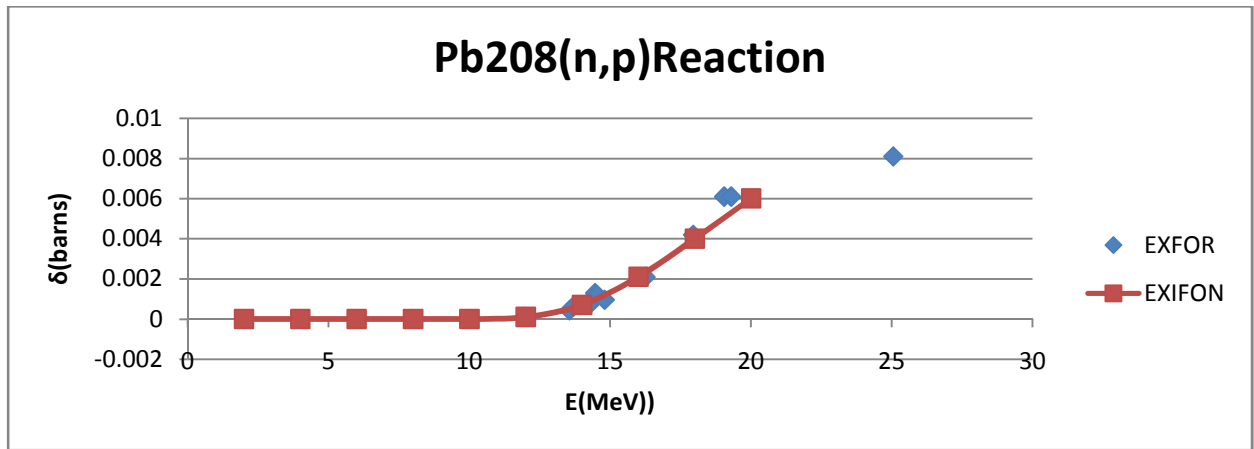


Fig. 4.9b

#### 4.10. Mg Nuclides

The stable isotopes for Mg are  $^{24}\text{Mg}$ ,  $^{25}\text{Mg}$ ,  $^{26}\text{Mg}$ , with isotopic abundance of  $^{24}\text{Mg}$  (78.99),  $^{25}\text{Mg}$  (10.00),  $^{26}\text{Mg}$  (11.01). The (n p) reaction channel of excitation functions for  $^{25}\text{Mg}$  nuclide shows disagreement between EXIFON and measured data, while those of  $^{24}\text{Mg}$  were partly in agreement. No data was found from measured data on  $^{26}\text{Mg}$ . Similarly the (n α) reaction channel for  $^{24}\text{Mg}$  were scanty and are in good agreement. While data for  $^{26}\text{Mg}$ ,  $^{25}\text{Mg}$ , from EXIFON were mostly in agreement measured data on that they are few and scanty.

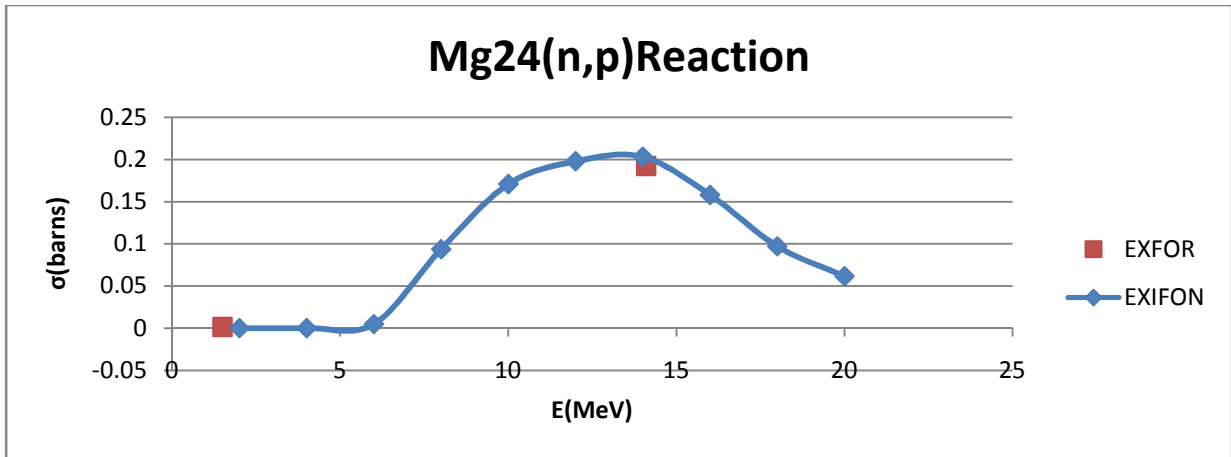


Fig. 4.10a

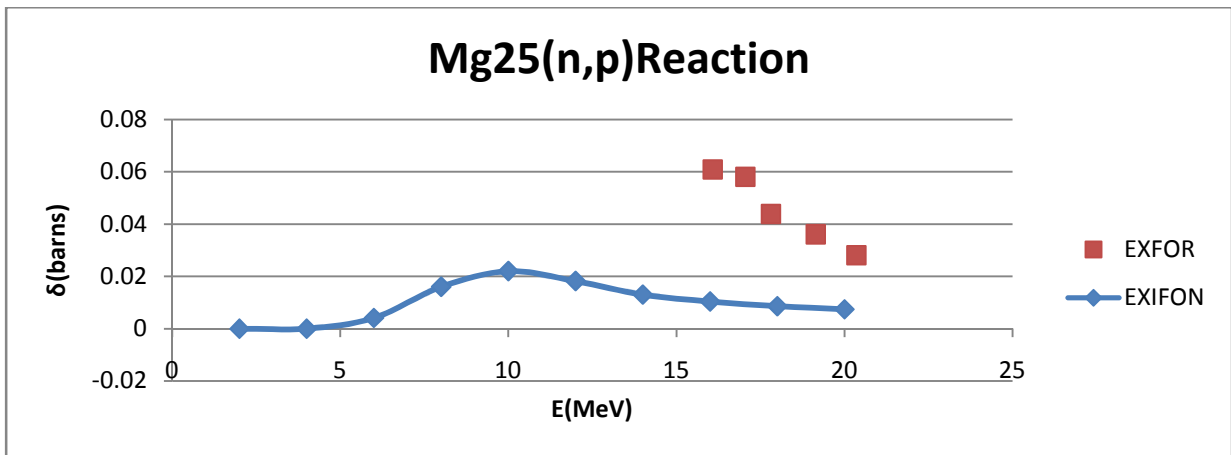


Fig. 4.10b

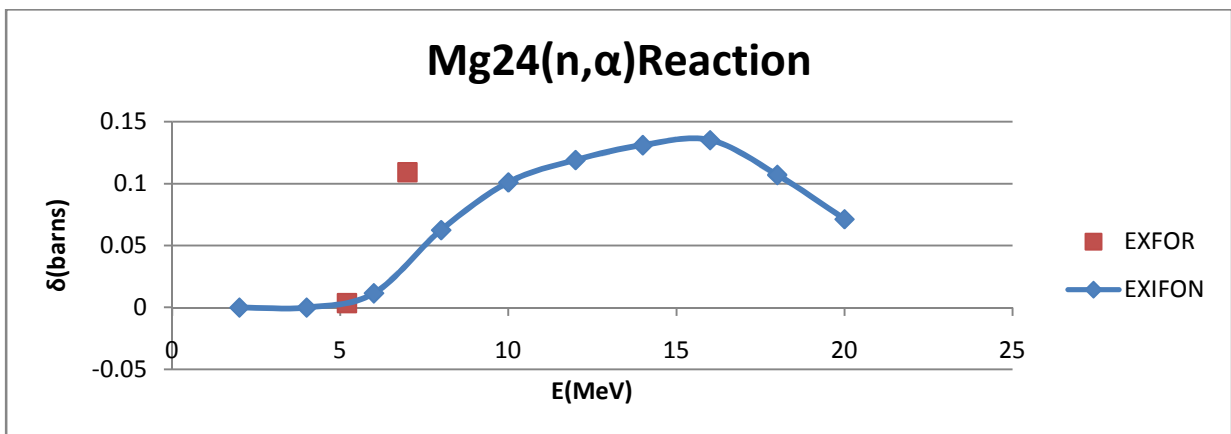


Fig. 4.10c

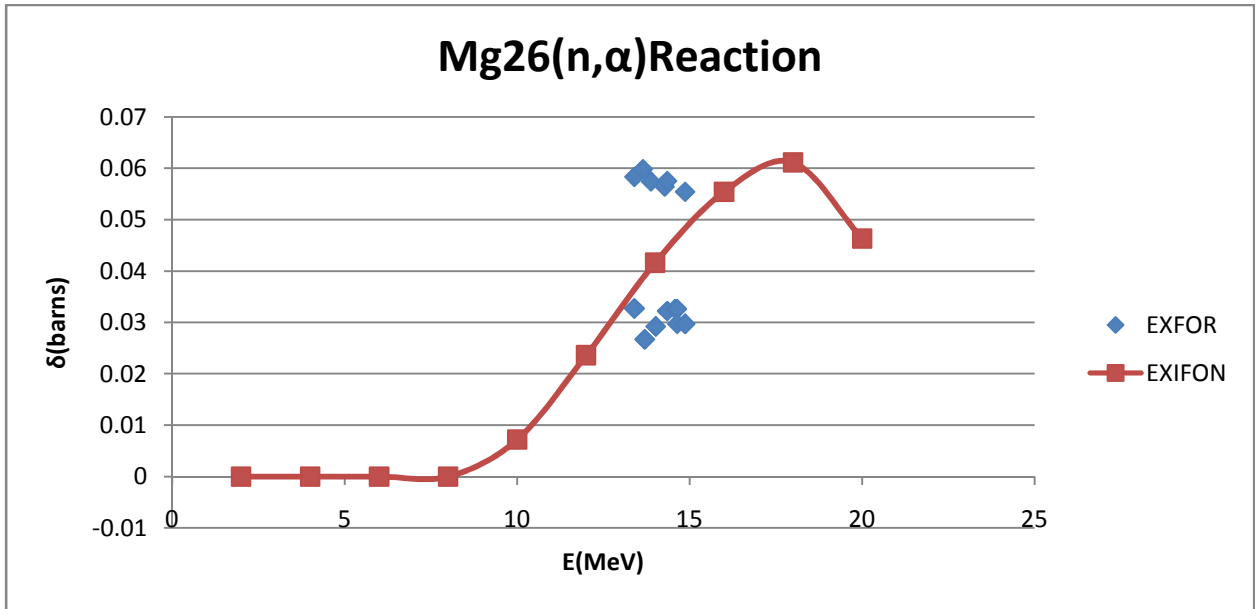


Fig. 4.10d

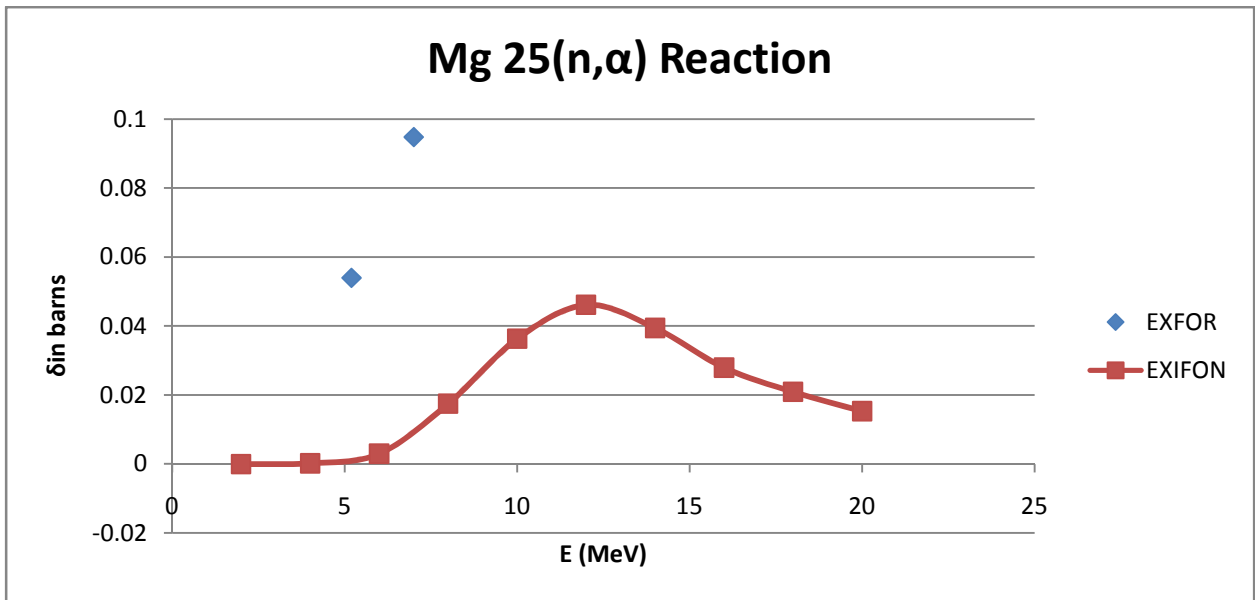


Fig. 4.10e

#### 4.11. Co Nuclide

$^{59}\text{Co}$  is the only stable isotope for cobalt with isotopic abundance of  $^{59}\text{Co}$  (100). The (n, p) reaction channel for  $^{59}\text{Co}$  shows good agreement between EXIFON and measured data around 13MeV – 18MeV. While the (n,  $\alpha$ ) reaction channel shows almost good agreement between EXIFON and measured data as well.

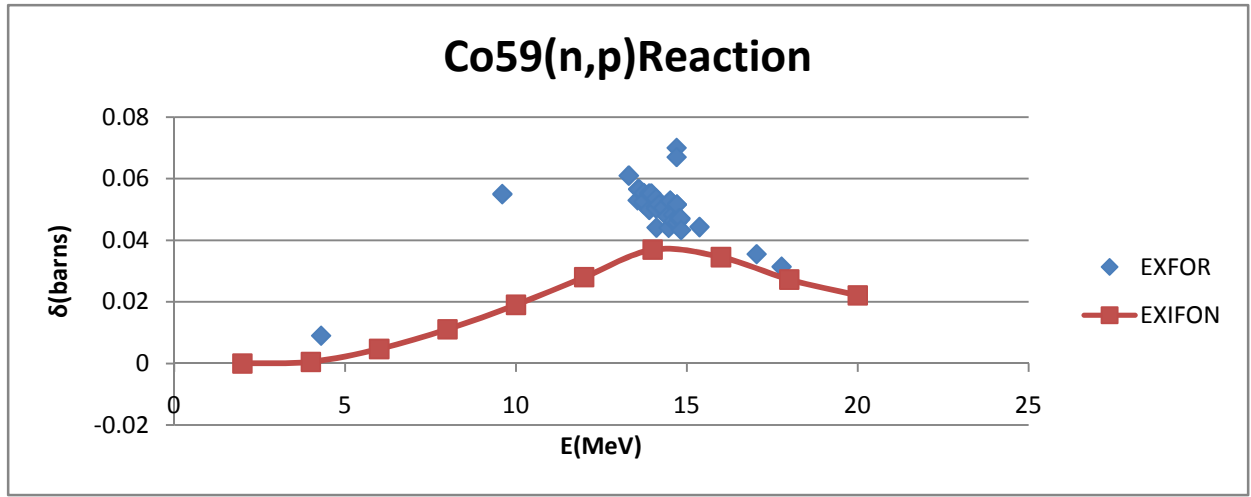


Fig. 4.11a

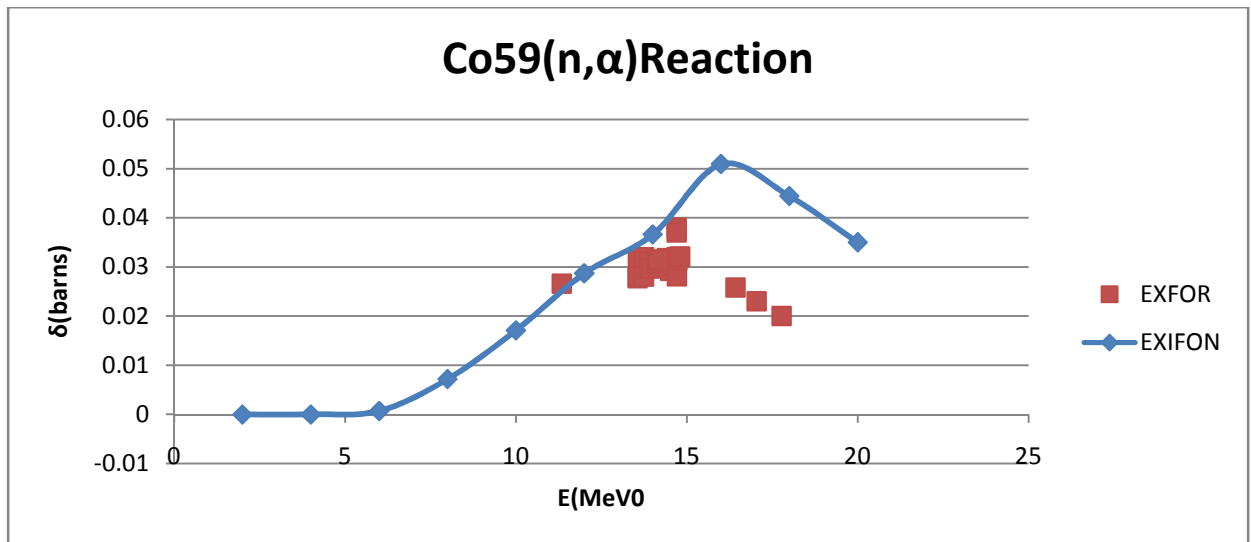


Fig. 4.11b

#### 4.12. Mn Nuclide

The only stable isotope for Mn is  $^{55}\text{Mn}$  with 100% isotopic abundance. (n, p) reaction channel shows almost good agreement between EXIFON and measured data. While for (n  $\alpha$ ) reaction channel EXIFON and measured data mostly are in good agreement around 6-10mev.

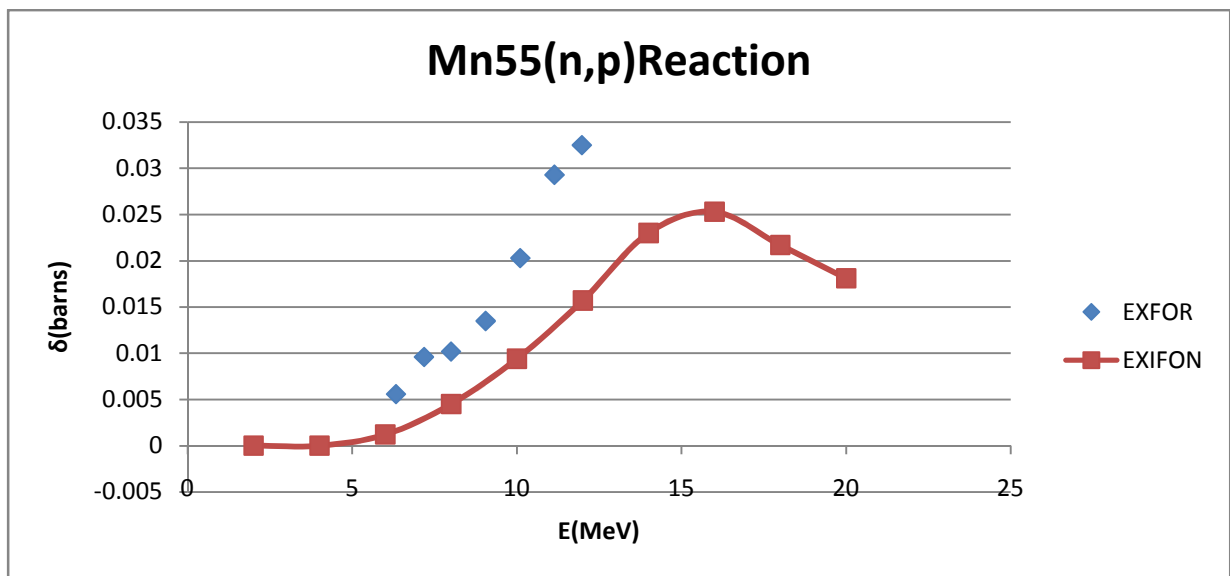


Fig. 4.12a

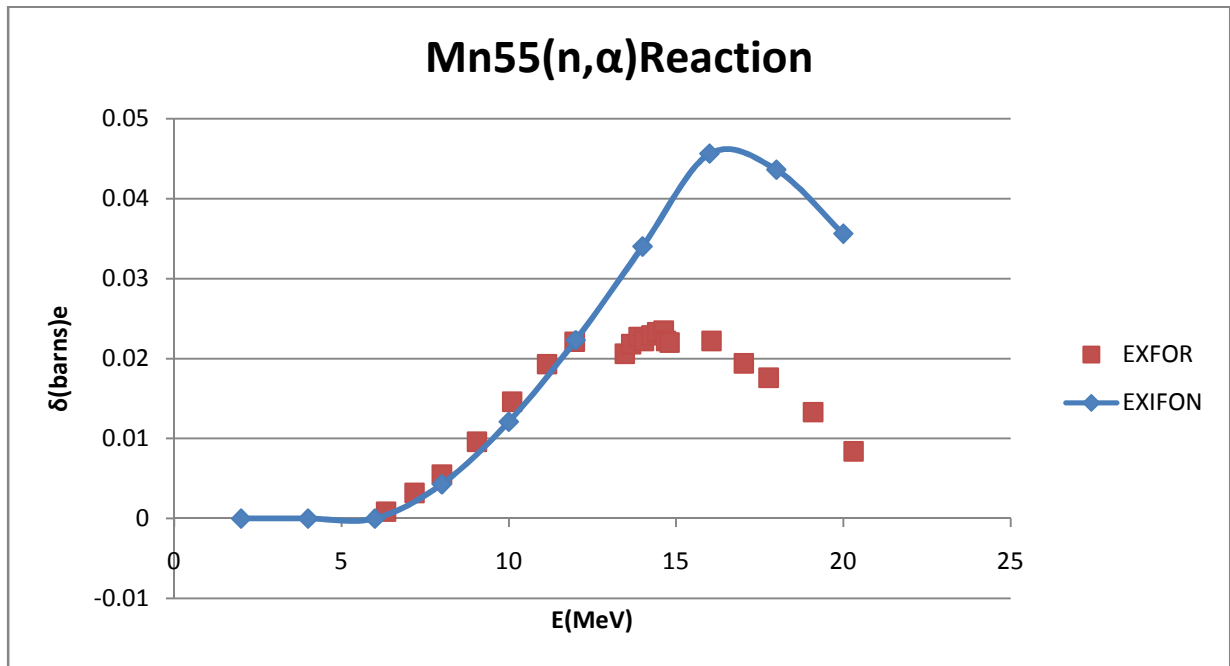


Fig. 4.12b

### 4.13. O Nuclides

The stable isotope of O are  $^{16}\text{O}$ ,  $^{17}\text{O}$ ,  $^{18}\text{O}$  nuclides with isotopic abundance  $^{16}\text{O}$  (99.70)  $^{17}\text{O}$  (0.038)  $^{18}\text{O}$  (0.200) and a concentration of 2500ppm. Being it the one with higher concentration on Be – reflector. The (n, p) reaction channel lacks data from measured data, while (n, α) reaction channel can be only able to account for  $^{16}\text{O}$ , in measured data library below 1MeV.

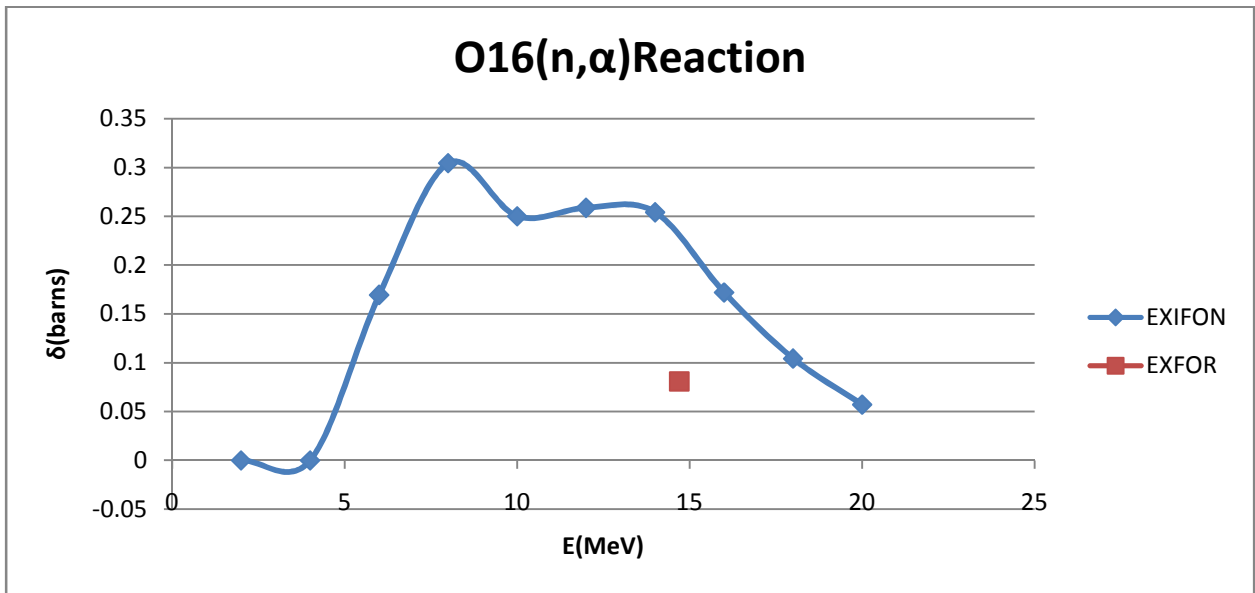


Fig. 4.13a

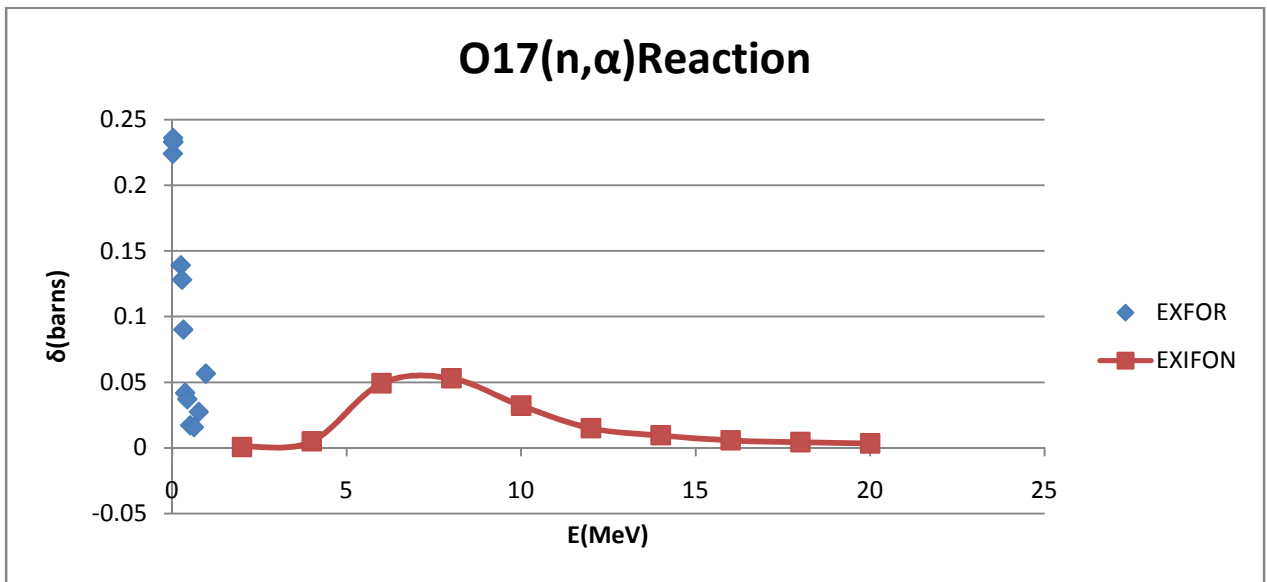


Fig. 4.13b

**A SUMMARY OF THE STATUS OF CALCULATED EXCITATION  
FUNCTIONS USING EXFOR AND EXIFON.**

Target Nucl ei	Percentage Isotopic Abundance (%)	Concentration in Part per million (ppm)	Status in EXIFON	Status in EXFOR		EXIFON Vs EXFOR (n.p)	EXIFON Vs EXFOR (n.α)
				(n.p)	(n α)		
<sup>54</sup> Fe	5.845	4000	Exist	Exist		Mostly agree	Agrees
<sup>56</sup> Fe	91.754	4000	Exist	Exist		Mostly agree	Agrees
<sup>57</sup> Fe	2.119	4000	Exist	Exist		Disagree	No data
<sup>58</sup> Fe	0.282	4000	Does not Exist	Exist	No data	No data	No data
				Exist	No data		
				No data	No data		
				No data			
<sup>27</sup> Al	100	3000	Exist	Exist		Agrees	Agrees
				Exist			
<sup>24</sup> Mg	78.99	1000	Exist	Exist		Agrees	Agrees
<sup>25</sup> Mg	10.00	1000	Exist	Exist		Disagree	Almost agree
<sup>26</sup> Mg	11.01	1000	Exist	Exist		No data	Almost agree
				Exist			Almost agree
				No data			
				Exist			
<sup>28</sup> Si	90.23	800	Exist	Exist	No data	Agrees	No data
<sup>29</sup> Si	4.683	800	Does not Exist	No data	No data	No data	No data
<sup>30</sup> Si	3.087	800	Exist	No data	No data	Agrees	Almost agree
			Exist	Exist			
				Exist			
<sup>58</sup> Ni	68.077	100	Exist	Exist		Agrees	Agrees
<sup>60</sup> Ni	26.223	100	Exist	Exist		Agrees	No data
<sup>61</sup> Ni	1.140	100	Exist	Exist	No data	Disagree	Almost agree
<sup>62</sup> Ni	3.634	100	Exist	data		No data	Almost agree
<sup>63</sup> Ni	0.926	100	Exist	Exist	No data	No data	No data
				data			No data
				No data			
				Exist			
				No data	No data		
				No data			
<sup>14</sup> N	99.634	200	Exist	Exist	No data	Incomplete	No data
<sup>15</sup> N	0.366	200	Does not Exist	No data	No data	No data	No data
				data			

<sup>63</sup> Cu	69.17	200	Exist	Exist	No data	Almost agree
<sup>65</sup> Cu	30.83	200	Exist	Exist Exist Exist		Mostly disagree
<sup>55</sup> Mn	100	200	Exist	Exist Exist	Disagree	Partly disagree
<sup>64</sup> Zn	48.63	150	Exist	Exist	Almost agree	Disagree
<sup>66</sup> Zn	27.90	150	Exist	Exist	Disagree	Almost agree
<sup>67</sup> Zn	14.10	150	Does not	Exist No	Disagree	No data
<sup>68</sup> Zn	18.75	150	Exist	data	Disagree	Mostly disagree
<sup>70</sup> Zn	0.62	150	Exist Does not Exist	No data No data Exist Exist No data No data	No data	No data
<sup>50</sup> Cr	4.345	200	Exist	Exist No	Agrees	No data
<sup>52</sup> Cr	83.789	200	Exist	data	Agrees	No data
<sup>53</sup> Cr	9.501	200	Exist	Exist No	Disagree	No data
<sup>54</sup> Cr	2.365	200	Exist	data Exist No data Exist Exist	Almost agree	Disagree
<sup>59</sup> Co	100	100	Exist	Exist Exist	Partly agree	Partly agree
<sup>16</sup> O	99.70	2500	Exist	No data Exist	No data	Incomplete
<sup>17</sup> O	0.038	2500	Exist	No data	No data	Incomplete
<sup>18</sup> O	0.200	2500	Does not Exist	Exist No data No data	No data	No data
<sup>204</sup> Pb	1.4	30	Exist	No data No	No data	No data
<sup>206</sup> Pb	24.1	30	Exist	data	No data	Agrees
<sup>207</sup> Pb	22.1	30	Exist	No data Exist	No data	No data
<sup>208</sup> Pb	52.8	30	Exist	No data No data Exist No data	Agrees	No data

## CHAPTER FIVE

### CONCLUSIONS AND RECOMMENDATIONS

#### 5.0: CONCLUSION:

The nuclear model calculations of excitation function were performed with theoretical model code EXIFON. Data of the excitation function were compared with measured data from IAEA-NDS EXFOR Data library. The theoretical code EXIFON adequately account for the interaction of nucleus with neutron in the energy range of interest. Results obtained differ from experimental data in the input parameter used in EXIFON code, which may not be able to account for structures of all the nuclides considered. For nuclides with magic number of neutrons or protons for example  $^{54}\text{Fe}$ ,  $^{16}\text{O}$ ,  $^{58}\text{Ni}$ ,  $^{208}\text{Pb}$  results obtained were found to be consistent with the experimental data.

The theoretical model code was able to predict the cross section data where no experimental data exist. In cases where the calculated data deviate significantly from experiments it is recommended to use other code that are robust and more flexible in terms of input parameter such as the EMPIR-II, ALICE and GNASH.

Another advantage of the theoretical model code, is that it was able to provide information of most of the cross section data for the nuclides of the impurities on the Be-reflector, where there are no measured data.

For the set of target nuclides in Be-reflector of NIRR1 experimental data EXFOR data were scanty and discrepant. Hence further measurements need to be carried out at different energies so as to improve data base. Most of measured data were around 14MeV.

The (n p) and (n  $\alpha$ ) considered in this work are to give information on the presence of H<sub>2</sub> and He gas formation on the Be reflector. With the exception of <sup>52</sup>Cr(n, p), <sup>53</sup>Cr(n p), and <sup>64</sup>Zn (n, p) reactions.

Finally, the EXIFON code adequately reproduce experimental data for the (n,p) reaction channel.

### **5.1: RECOMMENDATIONS:**

- a. Additional work are to be conducted for the experimental data to serve as a basis for comparison between measured data and theoretical code, in order to access the suitability of the theoretical model used.
- b. For other structural materials of NIRR-1, further research needs to be conducted on the activities of the impurities contained on these materials, so that it could give account of the integrity of the structural materials of NIRR-1.
- c. Hence a good knowledge of cross section data of all the structural materials of NIRR-1, need to be taken into consideration, even before the commissioning of NIRR-1.
- d. Similarly, the EXIFON code is suitable for the calculation of (n,  $\alpha$ ) reaction cross section except for <sup>68</sup>Zn, <sup>25</sup>Mg, <sup>55</sup>Mn, <sup>16</sup>O and <sup>17</sup>O

## REFERENCES

- Bernard L. Cohen (1971); Concept of Nuclear Physics. Tata.McGraw-Hill.New Delhi pp. 57- 105.
- G.I. Bologun, H.B. Garba, I.M. Umar, M.O.A Oladipo P.M. Egun, I.O.B. Ewa. I.I. Funtua, S. A. Jonah; A.M. Mati and Y.Fro. Nigerian Research Reactor 1. (NIRRI) first safety analysis. report. CERT/NIRR-I 001.Zaria Nigeria (2005).
- Hauser, W. and Feshback H. (1952); Inelastic scattering of neutrons, Physics Rev. 87. Pp. 366 - 373
- Hughes, D.J. (1957); On Nuclear Energy Oxford University Press London.
- Hughes D.J. (1957); Neutron Cross Sections International Series of Monographs on Nuclear Physics Pergamon Press New York.
- Kalka H. (1991); Exifon- A Statistical Multistep Reaction Code Report Technische University Dresden Germany
- Kalka H., Torgman, Lien H.N. Lopez, R and Seegler, D. (1990); Description of (n p) and (n 2n) Activation Cross Section for Medium Mass Nuclei within Statistical Multi Theory Z. Physics. A. Atomic Nuclei 335. 163 – 171.
- Pierre Marimier and E. Sheldon (1971) Physics of Nuclei and Particles. Academic Press Inc. London.
- P. Talou, m.B. Chadwick. F. Dictrech, M. Herman T., Kawanu, A. Koning, P. Ohion Zinky. (2004) “Sub Group A Nuclear Model Codes”. Report of the Sixteenth Meeting of the WPEC. France May 26 – 28
- S.A. Jonah (2005); Fission Neutron-induced analytical Sensitivities and Interference factors in N.A.A. with MNSR Reactors C.E.R.T. Abu. Zaria.
- S.A. Jonah (2004); Shell Structure Effect in Neutron Cross Section Calculation by theoretical Model Code Nigerian journal of Physics 16. (2)
- S.A. Jonah J.R., Liaw., J.E. Matos (2007); Monte Carlos simulation of Core Physics Parameters of the Nigeria. Research Reactor – 1 (NIRR 1) SCIENCE Direct. Annals of Nuclear energy 34 (2007) 9532957
- BV Calson (2001); A brief over few of models of nucleon induced reaction. Lectures given at work shop on Nuclear Data Science and Technology, Accelerators driven, waste incineration Trieste, 10-21 September.

O. Sehwerer (2001); A brief over few of models of nucleon induced reaction. Lectures given at work shop on Nuclear Data Science and Technology, Accelerators driven, waste incineration Trieste, 10-21 September.

M. Herman, R. Capote-Noye, P. Oblozinsky, A. Trkov and V. Zerkin (2002) Recent Development and validation of nuclear reaction codes. Journal Nuclear Science and Technology, supplement 2 p 116-119, 2002